



The
University
Of
Sheffield.

Department
Of
Mechanical
Engineering

MSc MECT53 Advanced Mechanical Engineering

Robotics: Actuator Gearbox Design for a brushless DC Motor

Ryan TANDY

August 2020

David Polson

Dissertation submitted to the University of Sheffield in partial fulfilment of the
requirements for the degree of Master of Science

Summary

With the increase in popularity of robotics in the hobbyist community—there is an increasing demand for low cost robotic components that are designed for robot build projects. One component in particular is the actuator. Actuators are a system typically made from a motor, a control system, and a gearbox. For robotics application, an actuator is the component which enables the motion of a robotic joint on a robotic arm for example. These components are often expensive for robotics due to the need for high-torque, high moment loading capacity, and compact design. As a result, hobbyists often use low-cost servomotors in their projects as an actuator—but these are designed for controlling the rudder on a model aircraft for instance. They are not designed to handle moment loads which robotic applications demand, so when used, the resulting structure is often weak and flimsy. The aim of this project then is to design a gearbox for an actuator which is designed to be low cost, compact, and have relatively high torque and moment loading capacity.

To achieve the project aim, the use of FDM technology was explored. FDM technology enables the manufacture of complex geometries for very low cost. One drawback is the polymers used for FDM are relatively low in strength compared to metals. This presented a significant design challenge to try and mitigate this drawback and create a successful design.

It was found that FDM was not suited to applications where the produced parts required high strength. As such—FDM is not good for manufacturing gears which need to simultaneously be small and handle large torques. This limits the use of FDM for gearbox manufacturing for robotic applications where space is often severely restricted. On the other hand, FDM was very successful at creating parts with complex geometries that would otherwise be hard to manufacture—and where strength is not an immediate concern. It is thought that when strength is a concern, a combination of machining and FDM methods to produce products is a good solution when cost is restricted as machining and FDM compliment each others' strengths while negating each others' weaknesses. This is considered to be the best direction on future work for successfully meeting the project aim.

Acknowledgements

I would like to thank my supervisor David Polson for his time, advice, and encouragement during the project. I would also like to thank him for giving me the opportunity to work on the project at very short notice.

COVID-19 Impact Statement

Unfortunately, the impact of COVID-19 was quite severe on the project itself. The project was arranged at the start of March (due to problems externally)—about a month before the university was forced to close. As a result, much of the early design work had to be revised due to unavailable manufacturing options. The design work then had to be completed alongside my other studies which made it quite difficult to progress. It then took a long time for the design to be manufactured as David was manufacturing the parts from home and sending them to me through the post; this was a slow process. This pushed back the intended schedule by months and as a result, there was not sufficient time to iterate the design and meet the project aim.

Despite the project aim being unfulfilled, it has to be said that the learning experience was still incredibly valuable to me. I was still able to experience the process of planning and developing a product—and my knowledge around the subject of robots, gearboxes, and 3D printing technology has increased significantly. So from this perspective, the situation regarding COVID-19 only had a minimal impact.

Chapter 1

Introduction

1.1 Robotics

The field of robotics is an interdisciplinary subject area at the interface between computer science and engineering. The term robotics encompasses the development and application of intelligent machines which are designed to automate tasks which would otherwise require a human to perform.

A robot differs from a machine in the sense that a machine has 'no brain'. A machine typically uses a source of electrical or mechanical power which moves certain components of the machine to perform some kind of useful movement. A desk fan is a good illustration of a machine; it uses electricity to power a motor which rotates the fan—creating a breeze. The fan cannot itself reverse the direction of rotation of the blades, nor can it stop rotating the blades while the electrical power is supplied to it. It cannot change the direction of the breeze—it cannot speed itself up or slow itself down. The only way to change the behaviour of the fan is to adjust the circuitry or components mechanically.

Contrast to that, a robot can intelligently perform a task based on the information it receives—either from a set of predefined instructions, user input, or information gathered by sensory equipment. A robot can decide how it operates at any point in time given its current state and objective. Robotic arms are a traditional example of a robot; an arm typically controls the motion of itself through use of a series of motors. These motors are instructed to speed up or slow down as necessary which allows the arm to move freely in space—something which the desk fan has no ability to do unless manually adjusted. A less obvious example of a robot is a home computer or mobile phone. Although they have no moving parts, they can perform a multitude of tasks autonomously, with user input, or even remotely. They may also 'learn' new tasks by installing additional software.

The function of a robot may be categorised as one, or a combination of five types [13]; pre-programmed, humanoid, autonomous, teleoperated, or augmented robots.

Pre-programmed robots rely on a set of pre-defined instructions to carry out simple and monotonous tasks. This type plays a major role in the manufacturing industry and are commonly used on assembly or packing lines. They are able to perform the

tasks faster, more accurately, for longer, and for a lower cost than a human could.

Humanoid robots are designed to mimic human behaviour and/or movements. These robots rely heavily on vast amounts of sensory data and complex artificial intelligence to operate since the environment they exist in is incredibly dynamic. The field of humanoid robotics is still largely academic—the extreme technological demands required by what we imagine as a humanoid robot cannot yet be satisfied by current technological development.

Autonomous robots are able to perform tasks without the need for an external operator. Similar to humanoid robots, these rely on sensory information and a more rudimentary form of artificial intelligence. Common uses for these types of robot are tasks which need to be performed on floor spaces and which take a long time. For example, floor cleaning or hoovering, lawn mowing, or painting marks (football field).

Teleoperated robots are user controlled. Commands are taken in real time and can be transmitted over a large distance so that the controller does not need to be present in the same location as the robot. These robots are commonly used to perform tasks in environments hostile to humans—such as underwater, in space, or high-radiation environments.

Augmented robots are designed to replace human capabilities that may be lost, or, simply to enhance them. This type of robot is usually either a prosthesis or exoskeleton. These rely completely on sensory information to move. This field is still in its infancy despite already having a tangible impact on people's lives.

Integrating a machine with a computer program provides extreme versatility from a design perspective—only constrained by current technological development—and has effectively limitless potential for applications.

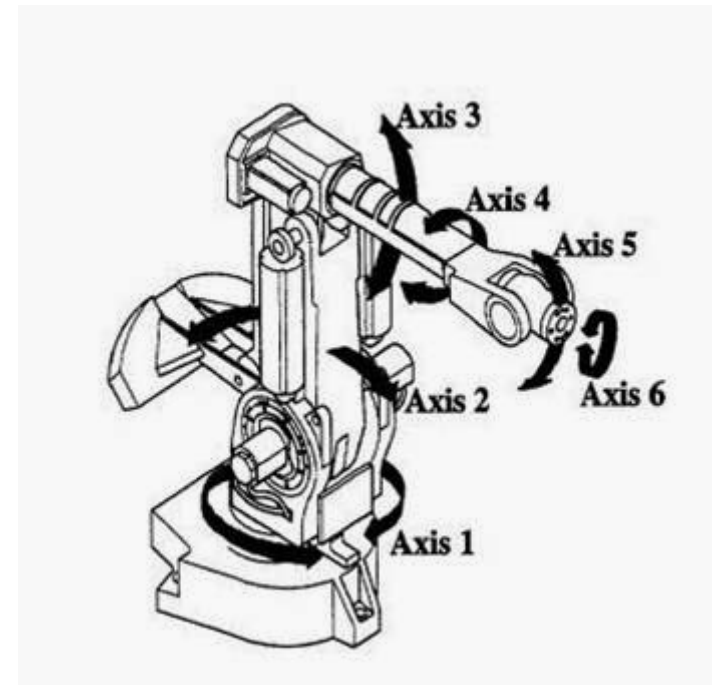


Figure 1.1: Robotic arm design which has six degrees of freedom [15].

1.2 The Project

For many types of robot—especially humanoid robots—dealing with moment loads on joints during operation (such as shoulder or elbow type joints) presents a significant design challenge as not only does the servomotor controlling those joints need to be strong unidirectionally, but the motor also needs to be compact and have a large output torque. It is also common to have servomotors attached in series—as seen in Figure 1.1—this creates additional demands on the motors as they have to support the weight



Figure 1.2: Left:- Dual shaft servomotor [21]. Right:- Servoblock exoskeleton [22].

of the arm in addition to the operational demands; any motor design therefore must weigh as little as possible. Additionally—due to the need for multiple motors, the cost may also quickly accumulate.

The consequence of designing such robots is that either: expensive servomotors that are designed to be compact and handle large moment loads are used—resulting in a very expensive robot; or, the structural strength and rigidity of the robot must be sacrificed to reduce costs.

With budget robots becoming more popular in the hobbyist community, there is an increase in demand for low-cost servomotors that are designed specifically for robotics—however, there are few options available. It is common for designs to use motors such as the one seen in Figure 2.3, but as mentioned earlier, these are not designed to handle moment loads. Additionally, their output torque is low so when these motors are connected in series—the result is a flimsy structure with a low loading capacity.

The best design solutions to meet this demand are dual shaft servomotors—which have two output shafts connected by a bracket—and servoblocks, which are a type of exoskeleton that attaches to a regular servomotor and increases the moment load capacity of the output shaft. These are shown in Figure 1.2. While these designs do greatly improve the structural strength of the motor, they do not improve the torque of the motor, they increase the cost (the servoblock is priced at \$30—more than the cost of the motor in most cases), and they increase the length of the motor—which is undesirable as this increases the stress on the fixings due to larger moments.

There is space for a servomotor design that is aimed at the hobbyist market—which is: compact, cheap, has a high output torque, and a high moment loading capacity; the aim of this project then is to fill the market gap.

The project attempts to mimic a servomotor by designing an actuator which consists of a gearbox, a brushless DC motor, a power supply, and an electronic speed controller. The design of the gearbox will be the key to producing a high torque and robust actuator. The plan to achieve this is to explore alternative manufacturing methods and design choices with the hope that they yield some interesting results.

More specifically—the use of filament deposition modelling (FDM), which enables the quick and cheap manufacturing of complex geometries—and alternatives to to bearings, which are often one of the components which drive up costs significantly.

Chapter 2

Background Knowledge

2.1 Actuators

Many robotic applications require complex motion to complete a particular task. Robots designed for these applications typically have some kind of arm that can freely move within 3-dimensional space. In order to achieve this, the arm needs 6 degrees of freedom—these are: up-down, forwards-backwards, left-right, pitch, yaw, and roll. There are a variety of engineering solutions which exist (ball joints, pulleys etc.)—however, the most common engineering solution is to design the arm with multiple joints which rotate or move in one plane or direction. Shown in Figure 1.1 is an example of a robotic arm design with six degrees of freedom.

The components which are responsible for the movement are called actuators. Actuators come in many different shapes and sizes, but they are classified as either linear or rotary, depending on their function. All actuators require a source of energy and a control signal, and will commonly use a motor to provide the motion—but may use an alternative instead, such as a hydraulic system.

2.1.1 Servo Motors

Servomotors are a popular choice of actuator for robotic applications. A servomotor is a device that allows for precise rotary motion. It is a closed-loop system which consists of a motor, a sensor, and some form of positional feedback. The servomotor takes an input signal for the desired angular position of the actuator; this input is converted to a pulse signal with a particular wave shape and period. The shape of the pulse is unique to a particular angular position. The servo system then uses a sensor and position feedback to minimize the error between the desired and current angular position of the actuator.

The performance of a servomotor is usually characterised by its torque, speed, degree of rotation (some servomotors may only have freedom to rotate 180° for example) and its power. These numbers can vary widely depending on the application the motor is designed for. As such, the price range is also wide. The most expensive motors are used for industrial robotics and can range in the thousands of pounds. These are

designed for large stationary robots that require a high amount of precision and speed, and where size and weight of the motor is not an immediate concern. These motors are also highly resistant to moment loads.

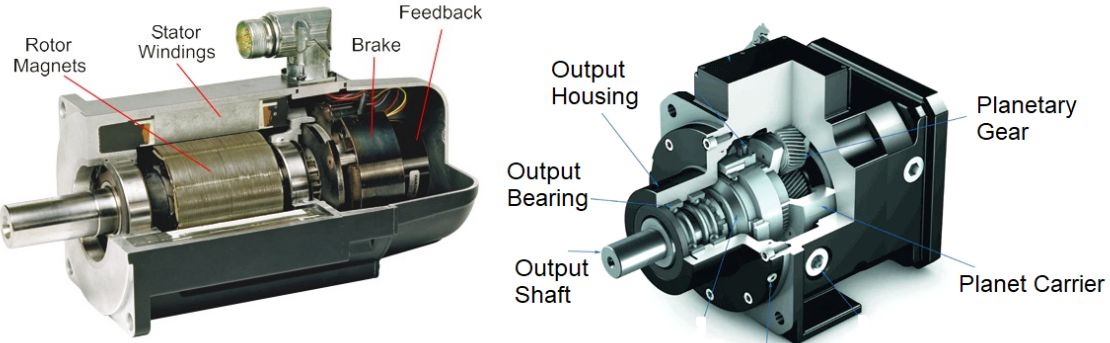


Figure 2.1: Left:- cut-away of an industrial servomotor [17]. Right:- cut-away of a planetary gearhead [18].

Servomotors typically require a gearbox so that the output torque of the actuator can be tailored to the application. This is often necessary so that the motor can operate within its optimal efficiency band. A gearhead can be fixed to the flange on the motor to achieve this. A typical gearhead for an industrial servomotor consists of one or more planetary gear stages and is designed to increase the output torque. More on planetary gear sets will be discussed later, but the main advantage of this type of gearing is that the load is distributed over more teeth—so the gearbox has a much higher load carrying capacity relative to other types of gearing. The inner workings of a typical industrial servomotor and planetary gearhead are shown in Figure 2.1.

On the other end of the price scale there are servomotors which have a price range between £10-30. The motors in this price range are typically designed for use in remote control vehicles for steering. A typical example of a low-cost servomotor is shown in Figure 2.3. For the cost, these motors are very well designed for their application. They are compact and good amount of torque—however, unlike the more expensive motors, they are not designed to handle moment loads.

2.1.2 Brushless DC Motors

Motors are the device that provides the motion for an actuator. They generate motion with a rotor which consists of multiple magnetic monopoles placed in a changing magnetic field. The magnetic field essentially pulls the rotor with it while the field itself is rotating.

Motors are categorized by the type of electrical power they use—either AC or DC—and also by their design; motor designs are usually referred to as either brushed, or, brushless motors.

A brushless DC motor consists of two components, a stator and a rotor. The rotor is the component that rotates—the stator is stationary. A schematic of a brushless DC motor is shown in Figure 2.2. Either the stator or the rotor may consist of permanent magnet (PM) monopoles—while the other consists of electro-magnet (EM) monopoles made from copper coils. If the rotor is on the outside of the stator, then the motor is referred to as an outrunner motor. Outrunner motors are the type commonly used for driving the prop shafts on model air planes and drones (See Figure 4.1 for an example of an outrunner motor). The EM pairs typically come in multiples of three—i.e. a rotor/stator may have three pairs or six pairs etc. Each pair is fed a different phase of power by an electronic speed controller (ESC). The ESC converts the DC power from the power supply into three phase power. The different phases create the rotating magnetic field by activating each EM pair at different times. The EM pairs are activated as they rotate towards the opposite polarity PM pairs—so the PM’s magnetic force pulls the EM’s towards them. As the EM’s pass the PM’s, the EM pair is deactivated so the PM’s magnetic force does not pull the EM’s back. The more EM pairs a motor has, the smoother the rotation is—and the faster the ESC changes the phases, the faster the rotor spins [51].

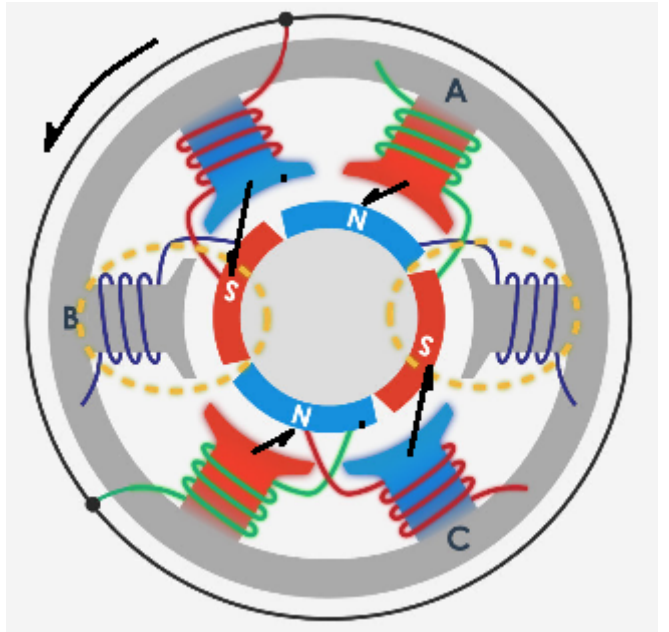


Figure 2.2: Schematic of a brushless DC motor [51].

2.2 Fused Deposition Modelling

Fused deposition modelling is a type of manufacturing process which builds parts layer by layer (referred to as additive manufacturing) as opposed to more traditional processes, such as material removal or moulding. FDM is done using a 3D printer. A 3D printer may come in a variety of shapes and sizes, but they all consist of a flat base, an extrusion nozzle, and a carriage which moves the nozzle around. In the case of a desktop 3D printer, a thermoplastic material (known as a filament) is fed into the nozzle where it is heated until molten—the nozzle then traces out a 2D cross-section of the part by depositing the molten filament onto the base. The filament then sets and the next layer is started. The 3D part is constructed by tracing out each 2D cross-section on top of the last. An image of a typical desktop 3D printer can be seen in Figure 2.4(a).

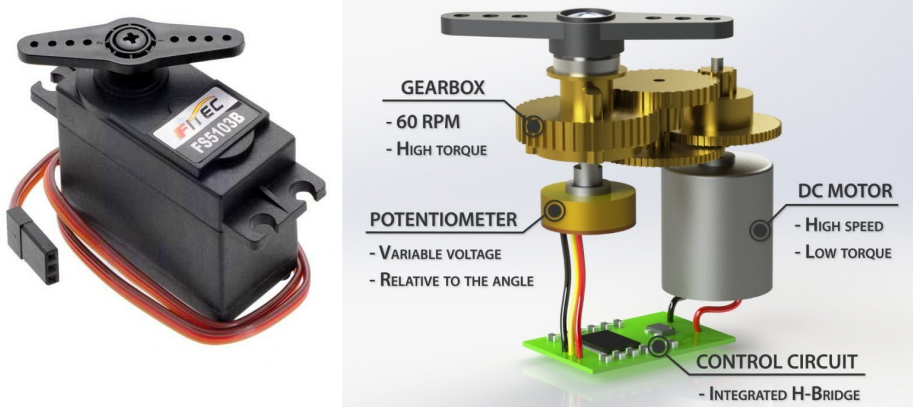


Figure 2.3: Left:- Example of a typical low-cost servomotor [19]. Right:- Internal view of the servomotor [20].

The defining feature of FDM is the ability to create components by decomposing complex 3D geometries into a series of simple 2D geometries. This enables the fast production of very complex components as a single piece of material. The big advantage of this is the reduction of interfaces which a component has; this both improves the problems associated with tolerance and leakage. It also reduces the amount of fixings required, lowering the cost. An example of this capability is shown in Figure 2.4(b).

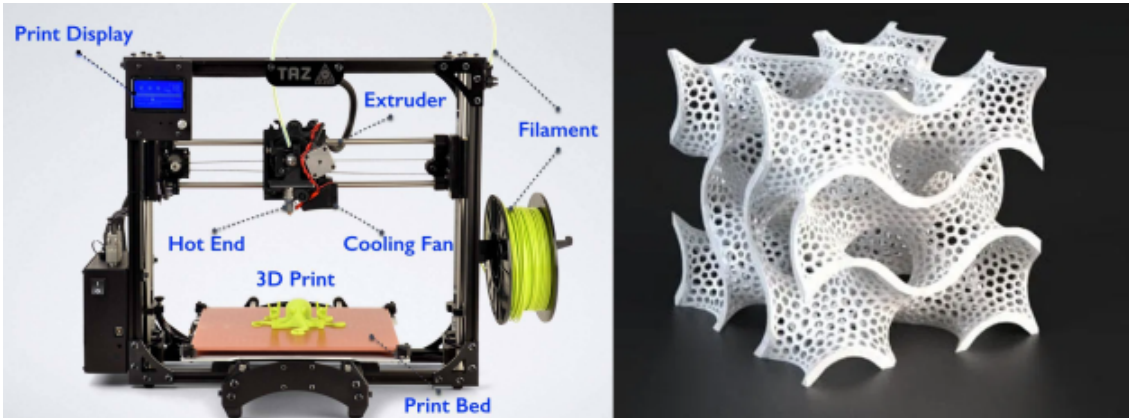


Figure 2.4: Left:- Components of a typical 3D printer [23]. Right:- Complex geometry made from a single piece of material using FDM technology [24].

2.2.1 Commercial Uses

FDM originally found use as a rapid prototyping technology after its inception in the 1980's. It enabled functional testing of new designs on the order of hours or days instead of weeks. However—since the turn of the century, there has been a growing interest in alternative commercial applications of FDM.

The field of architecture is one area that has seen a variety of novel applications for FDM explored. As well as rapid prototyping of architectural models—which are traditionally created by hand using organic materials such as wood or card—much research is being carried out on the application of the technology to build architecture projects.

Companies, such as Iconbuild [31], are using FDM to construct affordable housing using a specially designed concrete. It is claimed that this can reduce the cost of a house by 50%. An example of FDM technology used for construction is shown in Figure 2.5. Research published in 2018 [29] looks at the idea of combined 3D scanning and printing to model and replace deteriorating parts of historical buildings. A paper from 2017 investigates the use of FDM for repairing surface cracks to improve mechanical strength—stating that this could be especially useful for surface repairs of spacecraft in operation. Another example from 2013 [26] explores the application of FDM as a means to build a lunar base using material from the lunar surface. This would eliminate the need to transport large amounts of building material to the moon.



Figure 2.5: FDM technology used for construction [31].

There are many other areas that have also benefited greatly from the technology. In biomedical applications, the ability to print organs is becoming a reality. Examples of research have been highlighted in this article [32]—which include the creation of artificial vital organs, such as a heart, or a working pancreas for diabetic patients. Successful development of this technology will solve the shortage of organs currently experienced in the medical sector due to lack of donors. FDM has also revolutionised the field of prosthetics. One article [33] states that the technology has reduced the cost of new prostheses tenfold relative to traditional socket prostheses—and has also decreased the manufacturing time significantly. An example of these applications is shown in Figure 2.6. FDM has also seen use in the film industry for creating costumes and props, the aerospace industry for manufacturing lightweight components, and by hobbyists for a wide-variety of design and build, modelling, or art projects.

2.2.2 Polyactic Acid (PLA)

There are a wide variety of materials that exist for FDM manufacturing. Polymers are a popular option for desktop printing applications due to their relatively low melting point, durability, and low cost. The choice of material is a topic in and of itself—so an extensive discussion on material choice is omitted for brevity. A comprehensive



Figure 2.6: Left:-Bioink is injected into a hydrogel—creating a living tissue 3D printed heart [32]. Right:- Example of a low-cost printed prosthesis [34].

table of FDM materials and their properties can be found here [40]. However, due to the availability of materials for this particular project being limited to PLA, only the properties of this material are discussed.

PLA is generally regarded to be one of the stronger available polymers for FDM—but its reported ultimate tensile strength varies considerably depending on the source. For example, while [39] reports an approximate UTS of 65MPa, [40] reports a UTS of 50MPa and [41] reports the UTS to be much lower at 26.4MPa. This is likely due to inconsistencies between material composition of the manufactured test pieces (PLA often varies from manufacturer to manufacturer), but a safe assumption may be that PLA has a UTS on the order of tens of MPa. PLA is also a rigid material, but has low ductility. This makes the material prone to sudden fracture failure and surface damage from impacts.

One advantage of PLA is its low weight. The density of PLA is $1.24\text{g}/\text{cm}^3$ [53]. For reference, the density of aluminium is $2.7\text{g}/\text{cm}^3$ and the density of mild steel is $7.85\text{g}/\text{cm}^3$ [54]. This makes PLA a great choice for applications where very high strength is not a priority, but weight saving is.

One disadvantage is that PLA has a low melting temperature—between $150\text{-}160^\circ\text{C}$ [42]. While this helps to reduce the energy requirement for printing—it also implies that the maximum service temperature is low (52° [39]). This means that hot environments, or heat generation due to friction, could become a major issue—possibly even prohibiting the use of PLA altogether. The other issue with the low melting temperature is that during extrusion, PLA is prone to oozing and stringing. Cooling fans are required to help the PLA set quickly after extrusion. Layers that only require a small amount of material may cause the printer to print the next layer before the last has cooled sufficiently; this may lead to failed prints—as shown in Figure 6.5.

2.2.3 Print Optimization

As a consequence of the versatility and freedom to manufacture that FDM technology offers—naturally, 3D printers require numerous settings to be optimized in order to produce a successful print. Common parameters that need to be adjusted are: extrusion nozzle temperature, layer thickness, printing speed, filament flow rate, first layer height, infill pattern, bed surface, bed temperature, and retraction.

Extrusion Nozzle Temperature

The extrusion nozzle temperature controls the viscosity of the filament that is being deposited. If the filament is too hot, then the PLA will have difficulty holding its shape and begin to sag. The biggest issue with this is that it can lead to large deviations from the intended dimensions and result in parts that do not fit together. Another issue is that the filament will continue to ooze out from the nozzle over non-print areas. This causes the PLA to string across gaps, resulting in a messy print. The relationship between temperature and stringing demonstrated in Figure 2.7. On the other hand, if the temperature is too cool, then the new layer will have difficulty forming a strong bond with the previous layer. This can significantly diminish the structural strength of the printed part. The optimum temperature for the nozzle will depend on the speed of the nozzle movement and the layer thickness (which will affect the heat dissipation).



Figure 2.7: Shows the relationship between the extrusion nozzle temperature and filament oozing [45].

Layer Height

The layer height is the nominal thickness of a single layer of a 3D printed object. The layer height has a significant impact on the manufacturing time and quality of a product. A smaller layer height will improve the aesthetics of the print as the layered surfaces will appear smoother—but the parts will take much longer to print as there are more layers. An interesting finding is that for relatively thin parts, a smaller layer height will decrease the strength of the part by around 15% [47]. The research also finds that the strength of the print in the z-direction is around 20-30% weaker than in the other directions. The results indicate that the higher the total bonded surface area for a part is, the more likely it is to fail under a particular stress.

Infill Patterns

Infill patterns are often used to fill otherwise solid volumes in printed parts. The function of an infill pattern is to reduce the amount of material needed to fill the volume so that less material is needed, the time taken to print is reduced, and the weight of the part is reduced. The patterns are often used when the structural strength of a solid part is not required. The patterns are categorized by their appearance and the infill density—i.e. amount of material needed to print the pattern as a percentage of the material needed to fill the entire volume. Examples of different infill density are shown

in Figure 2.8. Research [47] shows that while different patterns exist, they are largely similar in their mechanical performance.

Filament Flow Rate

The filament flow rate is simply the amount of material that is extruded per unit time. The correct flow rate is dependent upon the speed at which the nozzle moves in space. It is also important to consider the nozzle temperature when changing the filament flow rate, as the higher the flow rate, the higher the temperature must be to melt the extruded material sufficiently [49].

First Layer Height

The first layer height is the height of the first printed layer. The distinction between the layer height and first layer height is necessary as the first layer height is almost always smaller. As the same amount of material is extruded to create the first layer as any other layer—the effect is that the material is squashed into the print bed by the nozzle and enables the first layer to stick to the print bed easier [49]. The downside to this is that the surface area of the first layer must increase; this can become an issue for parts printed with a tolerance—which may result in the material needing to be trimmed off for mating parts to fit together properly.

Bed Temperature

The bed is a—usually heated—flat plate that the first print layer is constructed on. Depending on the filament material, it may be necessary to heat the bed. Heating the bed prevents warping of the first layer as the molten filament—typically greater than 200°C—comes into contact with the otherwise relatively cold surface of the bed [49].

Retraction Controls

The retraction controls govern when, how fast, and how much filament is retracted back into the nozzle as the nozzle transitions between print and no-print areas. Retraction distance controls the amount of filament pulled back into the nozzle during a transition so that filament does not ooze out and string across discontinuities in the layer. The retraction speed controls how fast the filament is retracted. If the speed is too slow

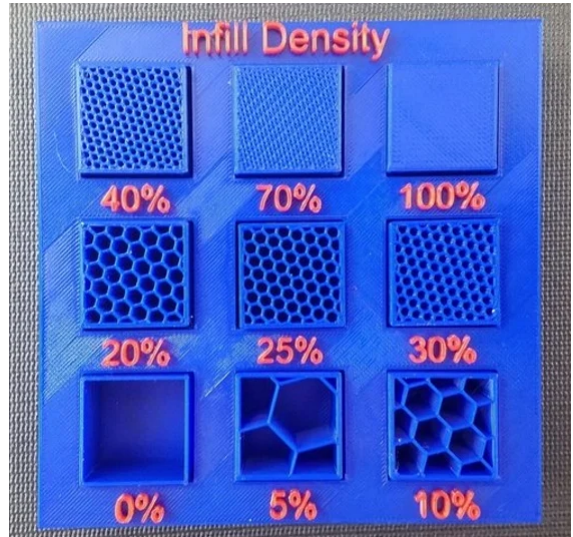


Figure 2.8: Examples of different infill density for a hex infill pattern [48].

then filament will continue to ooze out—again causing stringing effects. Coasting is the final retraction setting; this controls when the nozzle should stop extruding as the nozzle is about to reach a discontinuity. This is necessary as due to the nature of molten filament, there is an inherent time lag between when the printer stops extruding and when filament ceases to be deposited. The distance covered during this time delta is the coasting distance.

2.3 Tolerances

A critical part of the design process for manufactured parts is ensuring the correct tolerances are chosen. The concept of tolerance is simple: since it is impossible to manufacture the dimensions of parts with infinite precision—the tolerance is the acceptable error between a dimension of the manufactured part and its intended dimension.

Fit Types

Apart from making sure mating parts fit together, tolerances may also serve a secondary function. Tolerances are categorized as either: interference, clearance, or transitional [52]. If Δx is the tolerance gap between two mating edges—then loosely speaking, an interference fit is a negative Δx and a clearance fit is a positive Δx . A transitional fit is between interference and clearance. The fit types also have alternate descriptive names. Interference fits are referred to as push, or, force fits—transitional fits are referred to as sliding fits, and clearance fits are referred to as loose fits.

Fit types allow the designer to manufacture parts to achieve a particular function. The designer may want the two mating parts to hold together with friction, negating the need for adhesives and fixings; in this case—an interference fit is required. Two parts may need to fit together precisely, but need to reposition relative to each other—a transitional fit is the best choice to achieve this. It is also common for two mating parts to be required to not interact in any significant way so that they can move freely—or, the fit may simply be unimportant. Here, a clearance fit is the best choice.

Tolerance Interaction

When designing tolerances, it is vitally important to consider the interactions between tolerances. Tolerances may be specified such that they have a hierarchical structure. If this is the case, then the lower level tolerances may be overridden to ensure the higher level tolerances are not violated [52]. An example of this is illustrated in Figure 2.9. If the manufactured length of L is measured to be $L + .05$ —then this implies that the tolerance for K must change to $K_{-.05}^{+.0}$ so that the J tolerance is not violated. Therefore, it is important to be aware of such structures when designing the tolerances.

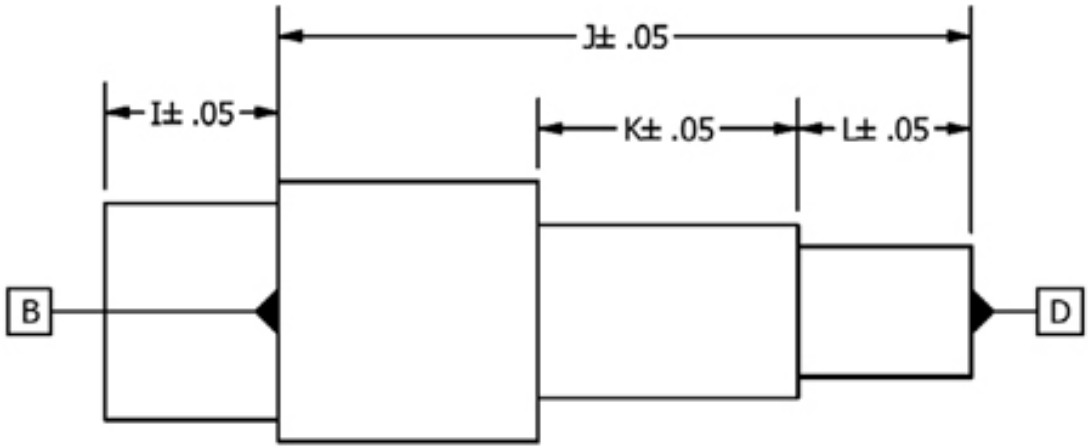


Figure 2.9: Example of a tolerance hierarchy [52].

2.3.1 Gearing

Gearbox design is a rich field in and of itself. A gearbox consists of a gear train—composed of a series of gears—an input shaft, at least one output shaft, and a casing. Gearboxes may serve one or multiple functions; these functions are: changing the speed and torque, changing the direction of power transmission, reversing the direction of rotation, or synchronizing the rotation between multiple outputs.

Gear trains may be composed of a variety of gear types—each with a unique function—and there are infinitely many ways to combine them to produce a gearbox which is perfectly tailored to its application. The most common types of gear are shown in Figure 2.10.

Spur gears have a 2-dimensional profile which is extruded in the third dimension. The line of contact between two meshed spur gears is always parallel to the axis of rotation. Spur gears are useful because they are the cheapest and easiest type of gear to design and manufacture. They have a higher power transmission efficiency than any other gear type and the velocity ratio is constant. The main disadvantages are that spur gears are noisy at high speeds, they can not transmit power in the axial direction, and the gear teeth experience high stresses.

Helical gears are similar to spur gears—the distinction is that the shape is generated by rotating the 2-dimensional profile at a linear speed during extrusion. As a result, the teeth ridges follow a helix trajectory; this changes the direction of the line of contact so that it is no longer parallel to the axis of rotation. The advantage of this is that it reduces the bending stress on the gear teeth by deflecting part of the transmitted force along the width of the tooth. The disadvantage to this tooth shape is that the act of deflecting the transmitted force produces thrust in the axial direction; this increases heat generation and reduces power transmission efficiency. Double helical gears are designed to tackle this issue by generating equal and opposite thrust in each direction.

Other advantages and disadvantages are that helical gears produce less noise, but are more difficult to design and manufacture—thus, are more expensive.

Bevel gears consist of two conical mating gears which have non-parallel axes of rotation. They are primarily used to change the direction of power transmission. The gears may have either straight or spiral teeth, analogous to the spur and helical gear. The mating pair of gears need not have the same number of teeth so bevel gears can be used to change the transmitted speed and torque. Miter gears are the special case of bevel gear where the mating gears have an equal number of teeth and the axes of rotation are perpendicular—thus, are used only to change the direction of power transmission.



Figure 2.10: Common types of gears [16].

The worm gear is essentially a helical gear with a high helix angle which mates with a spur gear. Advantages include: silent operation, effectively zero backlash, and the ability to reach very high ratios within in a single stage. The main disadvantage of worm gears is exposure to friction and stress. This requires the gear material to have a high resistance to surface wear, low coefficient of friction, and high yield strength. This limits the choice of suitable materials.

Internal gears are essentially inverted spur gears—therefore, share the same advantages and disadvantages. This type of gear is commonly used as a space saving device since one of the mating gears is located within the circumference of the other, which reduces the footprint of the mating pair.

2.4 Bearings

Chapter 3

Background Theory

3.1 Gear Theory

3.1.1 Terminology

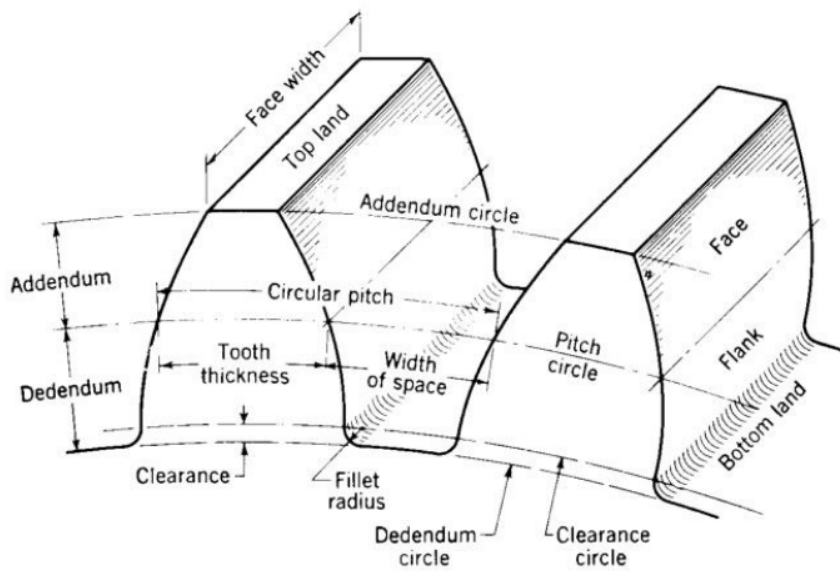


Figure 3.1: Nomenclature for spur gears [1].

Term	Meaning
Pitch Circle	The imaginary circle which is tangent to the pitch circle of another meshing gear. Defines the contact radii of two gears.
Diametral Pitch	The ratio of the number of teeth on a gear and the diameter of its pitch circle.

3.1.2 Basic Gear Trains

The most basic example of a conventional spur gear train consists of two gears where their pitch circles are tangential to each other—shown in Figure 3.2. The smaller gear is known as the pinion and the larger gear is known as the gear. For a reduction gear train, the pinion is the drive gear.

Gear Ratio

The gear ratio i is defined as the factor by which the angular velocity of the driven gear ω_2 must be scaled by to match the angular velocity of the drive gear ω_1 [58]—i.e.,

$$\omega_1 = i\omega_2 \quad \Rightarrow \quad i = \frac{\omega_1}{\omega_2}; \quad (3.1)$$

if $1 < i$, then the gear train is a reduction gear train. Alternatively, the gear ratio can be written in terms of the gear diameters as

$$i = \frac{d_2}{d_1}. \quad (3.2)$$

Here, d_j is the diameter of the pitch circle of gear j . This stems from the fact that the gear teeth impose a no-slip condition between two meshed gears. Then the linear velocities of two meshed gears is equal—i.e., $v_1 = v_2$. Since angular velocity is defined as $\omega_j = v_j/r_j$ —substituting ω_j for v_j/r_j into (3.1) yields the result.

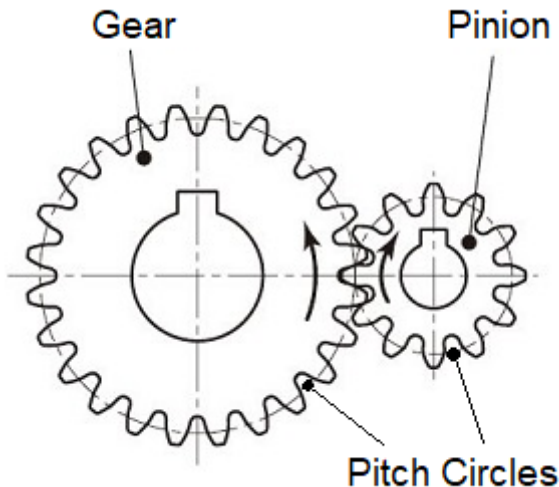
This implies that a fundamental limit exists on the maximum ratio that is able to fit within a given area. The minimum rectangular area

$$A_{min} \approx d_2(d_2 + d_1), \quad (3.3)$$

The only way to increase the ratio of the gear train without significantly increasing the area is to extend the gear train in the axial direction. However, the area would still require an increase to

$$A_{min} \approx d_2 \left(d_2 + \frac{1}{2}(d_2 - d_1) \right), \quad (3.4)$$

Figure 3.2: Basic example of a gear train [6].



in order to be an efficient solution (see Appendix 1 for further explanation).

Tooth Bending Stress

The Lewis Equation is the classical method for estimating the stress at the root of the tooth under load [11]. The equation is expressed mathematically as

$$\sigma = \frac{W_t P}{F Y}, \quad (3.5)$$

where W_t is the tangential load on the tooth, P is the diameter of the pitch circle, F is the face width, and Y is the Lewis form factor (LFF). The LFF is a scalar quantity that depends on the tooth profile—which is itself related to the number of teeth on the gear; tables for various values can be readily found in the literature [11]. It is widely accepted that if the Lewis stress σ is less than a third of the UTS of the material, then the gear teeth should not fail due to bending stresses. N.B. The Lewis equation does not account for surface failure due to wear—in this case, it is necessary to use the modified Lewis Equation if wear is anticipated as a significant factor.

Force Transmission

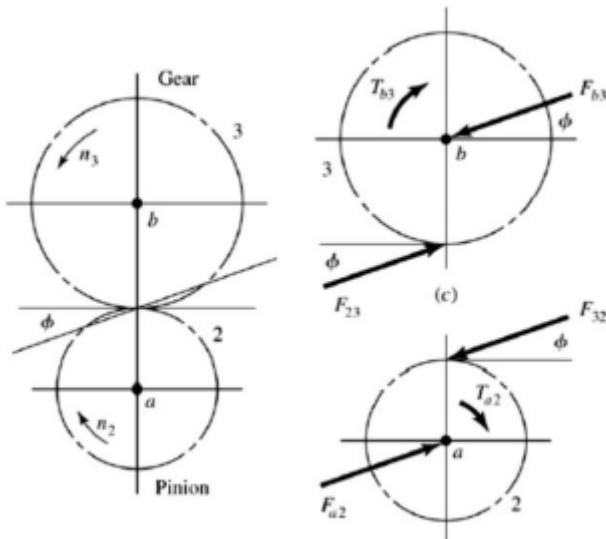


Figure 3.3: Free body diagram of a basic gear train [12].

Number of Teeth

The number of teeth on a gear z is a free choice for the designer. However, appropriate choices for z depend on the operating conditions. For gear rotating at high speed, z should be larger—this is due to the generation of heat by friction which must be dissipated and also to decrease the wear on any individual tooth. For gears exposed to large loads, z should be smaller so that the individual teeth are stronger.

The number of teeth is related to the diameter by the circular pitch p —i.e.,

The torque τ transmitted from the driving gear to the driven gear is proportional to the gear ratio—expressed as

$$\tau_1 = i \tau_0. \quad (3.6)$$

This result is derived from the fact that the torque is proportional to the radius of the gear—i.e., $\tau_j = F_j r_j$, where F_j is the transmitted force; as $F_0 = F_1$ since the transmitted force is constant, then $\frac{\tau_1}{\tau_0} = \frac{r_1}{r_0} = i$. A force analysis for the basic gear train is shown in Figure 3.3. The bearing forces are equal and opposite to the forces experienced by the gear teeth.

$$z = \frac{\pi d}{p}. \quad (3.7)$$

Module

The module of a gear is a geometric property that describes whether two gears will mesh. It is defined as the ratio between the diameter and number of teeth of a gear—i.e.,

$$m = \frac{d}{z}. \quad (3.8)$$

If two gears share the same module, then they will mesh correctly.

3.1.3 Planetary Gear Trains

A planetary gear set is an alternative configuration for a gear train where the pinion is located within the circumference of the gear. A typical example of a planetary gear set is shown in Figure 3.4. The planetary gear set consists of three parts: a sun gear, a planetary carrier with planet gears, and a ring gear. One of these parts must be held stationary while the other two act as either the drive or driven gear. For a reduction gear set, the sun gear is the drive gear and the carrier usually acts as the driven gear; occasionally, the ring gear is the driven gear.

One advantage of a planetary gear set is that it effectively reduces the minimum area of the gear train to

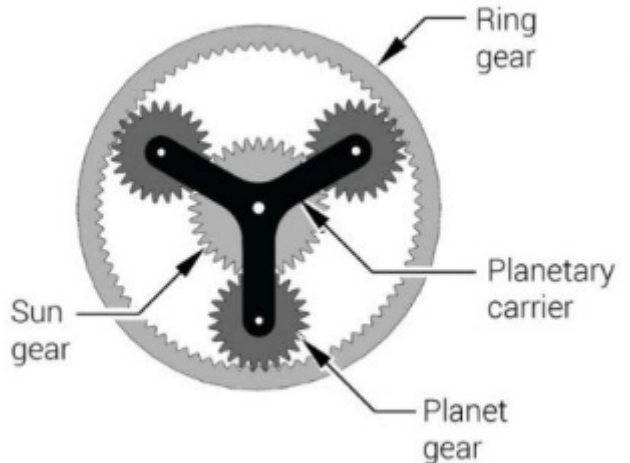


Figure 3.4: Example of a planetary gear set [7].

$$A_{min} \approx d_R^2 \quad (3.9)$$

where d_R is the diameter of the ring gear pitch circle. Additionally, planetary sets can also be extended in the axial dimension and maintain efficiency without increasing the minimum area.

Planetary Gear Ratio

The gear ratio of a planetary set depends on which part is fixed, and which part is the driven gear. For a reduction gear train, if the carrier is fixed, then the gear ratio is [59]

$$i = \frac{d_R}{d_S} \quad (3.10)$$

where d_S is the diameter of the sun gear. However—if the ring gear is fixed and the carrier acts as the driven gear, then the gear ratio becomes [59]

$$i = 1 + \frac{d_R}{d_S} \quad (3.11)$$

This particular configuration yields an increase in the gear ratio without changing the dimensions of the gears. The formal explanation is omitted for brevity (see here for a full explanation [8])—but the increase in ratio appears due to the additional rotation of the planetary carrier as the planet gears rotate. The planetary set effectively has two drive gears which contribute their combined linear velocities to the driven gear. This is another major space-saving advantage relative to the basic gear train.

Number of Teeth

The number of teeth for each gear in a planetary set can be calculated using the following relations:

$$z_R = z_S + 2z_P; \quad z_R = \frac{d_R}{d_S} z_S. \quad (3.12)$$

Interference

It is possible to choose the number of planet gears within a set, depending on the application. Commonly, sets use three planets—however, for lower ratios, it is possible to fit six planets. For high speed applications, it may be desirable to have only two planets so that friction and heat generation is reduced—but for high torque applications it may be desirable to choose a greater number of planets so that the load is distributed over more teeth.

It is not always possible to equally space planets without interference between the teeth—therefore, the following formula is used to determine whether the number of planets selected for the set is permissible [60]:

$$I = \frac{z_S + z_R}{P_n}. \quad (3.13)$$

Here, z_R is the number of teeth on the ring gear, z_S is the number of teeth on the sun gear, and P_n is the number of planets. If I is an integer value, then there is no interference between the teeth.

3.1.4 Gear Efficiency

There are a variety of factors which affect the efficiency of a gear train—these include: wind-up, backlash, undercutting, bearing friction, pitch angle, and number of components. Since it is difficult to quantify the effect of these factors on the efficiency of the gear train individually, these contributions are typically combined as an efficiency factor η such that

$$p_1 = \eta p_0; \quad \eta_g < 1, \quad (3.14)$$

where p_0 is the power in and p_1 is the power out. The efficiency factor must then be measured experimentally. The quantity

$$\phi = p_0 - p_1 \quad (3.15)$$

measures the power losses due to gearbox inefficiency.

Increasing Gearbox Efficiency

Wind-up: defined as the kinetic energy losses due to torsion. When under load, gears experience torsion—which converts kinetic energy into potential energy stored in the material; this results in a loss of motion. Using materials with a high Young's modulus is the best way to reduce wind-up.

Backlash: described as the arc-length that a gear can rotate before contacting another meshed gear. This 'looseness' results in a loss of motion, a decrease in smoothness of rotation, and a decrease in precision [61]. The application depends on the amount of acceptable backlash—e.g., robotics applications often require a high amount of precision and so backlash much be minimized as much as possible (typically < 3 arc min); toy designs, such as the gearbox in a remote control car, do not require this level of precision.

Some backlash is often desired according to Hatch [9]; it is often necessary to allow space for lubrication, thermal expansion—and depending on the application, if there is a likelihood of shock loads or jams for instance, then backlash helps to decrease the possibility of damage to the gears. The main source of undesirable backlash comes from manufacturing tolerances. Therefore, backlash is totally dependent on the manufacturing process selected.

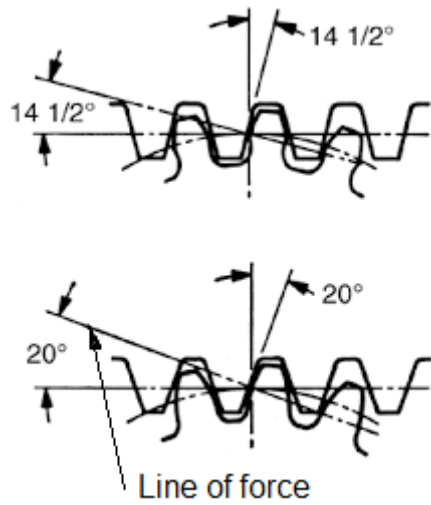


Figure 3.5: Shows the line of force for two pitch angles; 14.5° and 20.0° [10].

21

Pitch angle: this is the angle at which the force is transmitted from one gear to another (line of force)—shown in Figure 3.5. Decreasing the pitch angle increases the tangential force component and decreases the normal force component—thus, increasing the transfer of torque. However, decreasing the pitch angle also increases the stress in the gear teeth. Standard pitch angles for gear design are 14.5° and 20° , but 14.5° has lost popularity over time in favour of 20° which offers a better compromise between efficiency and tooth strength.

Undercutting: this is a process that happens when the number of teeth on a gear is low; the tips of the teeth on a gear will interfere with the base of the teeth of the meshed gear. To avoid wear, the base of the teeth are filleted—but doing so reduces the strength of the teeth as material must be removed. Boston [10] states that to avoid interference, 32 teeth are needed on a gear with a 14.5° PA and 18 for a 20.0° PA.

Planetary Gear Ration and Efficiency

The efficiency of a gear is related to the number of teeth it has. Undercutting and excessive backlash occur when a gear has a low number of teeth; both contribute to loss of power. Improving efficiency is then a matter of designing gears with as many teeth as possible while keeping the teeth to be large enough to maintain sufficient strength for operation. More teeth also reduces the effect of surface wear and stress on any individual tooth, increasing lifespan.

The efficiency of a planetary set is determined by the number of teeth on the smallest gear in the set. If the diametral pitch of the ring gear is fixed, then the diametral pitch of the sun and planet gears will vary with the gear ratio. The higher the ratio, the larger the planet gears become; the sun gear must get smaller to compensate. If the tooth size is also fixed, then the number of teeth on the sun and planet gears will vary too. This effect is shown in Figure 3.6. Typically—as the ratio increases, the number of teeth on the smallest gear decreases. For a 4:1 gear ratio, the number of teeth on the smallest gear is maximised. The peak appears for the same reason that the area of rectangle is maximised when the side lengths are equal. For ratios lower than 4:1, the planet gears are smaller than the sun gear—but for ratios higher than 4:1, the sun gear is the smallest gear. A ratio of 4:1 implies the sun and planet gears are equal in size. The figure then shows that when space is restricted, a 4:1 ratio offers the highest efficiency.

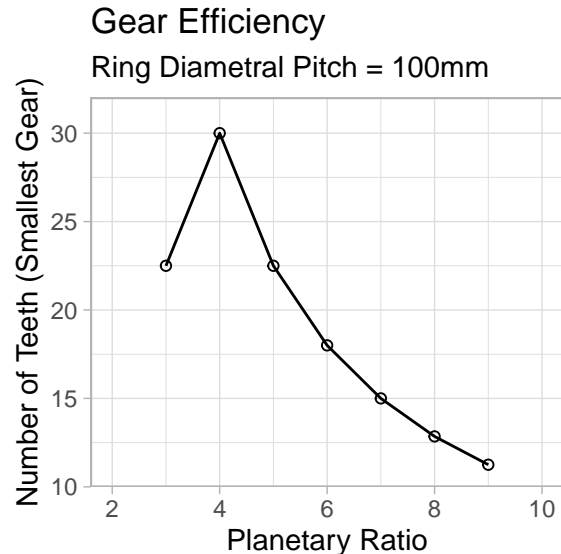


Figure 3.6: Shows the relationship between the ratio of a planetary gear set and the number of teeth on the smallest gear—for a fixed ring gear diametral pitch and fixed tooth size.

3.2 Motor Theory

The performance of a motor can be characterised by taking measurements of various performance markers and modelling their relation to the torque.

Torque-Current

The relationship between torque and current is useful to understand how hard a motor has to work at a particular load. The torque produced by a motor during operation requires a certain amperage draw. This amperage draw can exceed the maximum continuous current threshold if the operational demands are sufficiently high—in which case, the motor cannot run continuously without the risk of suffering thermal damage.

The model for the torque-current curve is

$$\tau(I) = K_t(I - I_0), \quad \tau \geq 0, \quad (3.16)$$

where I is the current, I_0 is the idle current, τ is the torque, and K_t is the torque constant. The idle current is the amperage draw required by an unloaded motor to spin and accounts for energy loss due to hysteresis (iron loss (φ)) and bearing friction. The torque constant is inversely proportional to the K_v rating of a motor in the following way:

$$K_t = \frac{60}{2\pi K_v}. \quad (3.17)$$

The maximum/stall torque can be found from (3.16) using the stall current (I_s)—i.e., the maximum amperage draw of motor; this occurs when the rotor is physically stopped from spinning. The stall current is calculated from Ohm's Law [55]:

$$I = \frac{V}{R}. \quad (3.18)$$

Here, R is the resistance in the copper windings and V is the potential difference across the motor circuit. A spinning motor generates an electromotive force (voltage) due to the changing magnetic flux in the windings (Lenz's Law [56]) which opposes the input voltage; this is called the back-emf. The current then depends on the difference between the input voltage (V_0) and back-emf (ε)—i.e,

$$I \propto V_0 - \varepsilon. \quad (3.19)$$

Therefore, I_s is obtained from (3.18) when $V = V_0$ ($\varepsilon = 0 \Rightarrow$ stationary rotor).

Torque-Speed

The rotational speed of a rotor (ω) is negatively proportional to the torque. The general model for the speed-torque curve is

$$\omega(\tau) = \omega_0 - \frac{\Delta\omega}{\Delta\tau}\tau; \quad (3.20)$$

ω_0 is the no-load speed—the theoretical maximum speed of an unloaded rotor. A convenient substitute for $\frac{\Delta\omega}{\Delta\tau}$ is $\frac{\omega_0}{\tau_0}$ where τ_0 is the stall torque. The no-load speed is simply the product of the input voltage and the K_v rating;

$$\omega_0 = K_v V_0. \quad (3.21)$$

Torque-Power/Efficiency

A motor converts electrical energy mainly into mechanical and thermal energy. The conversion of electrical power to mechanical power is a measure of a motor's efficiency (η) [57]. Expressed as

$$\eta(P_m, P_0) = \frac{P_m}{P_0} \quad (3.22)$$

where P_0 is the input power and P_m is the mechanical power output. Here, $P_0(I) = IV_0$ and P_m is simply the product of the speed and torque—

$$P_m(\tau, \omega) = \tau\omega. \quad (3.23)$$

The power that is not converted to motion is instead converted to heat due to the resistance in the copper windings, known as copper loss (ϑ). The copper loss is the difference between the electrical power and the mechanical power:

$$\vartheta(P_0, P_m) = P_0 - P_m. \quad (3.24)$$

Chapter 4

Design Task

4.1 Project Aim

Design a low-profile, high-reduction gearbox for an outrunner motor which is low cost and easy to manufacture.

4.2 Milestones

4.2.1 Literature Review

This will encompass all the necessary learning of theory and pre-requisite knowledge that needs to be understand to carry out the project—and also to investigate existing projects and products which share a similar goal to this one.

The theoretical knowledge will include:

- **Motor theory.** How the motor performance and efficiency can be estimated. This will help determine how the motor will perform under particular loads; the information can then be used to select an appropriate gear ratio.
- **Gear theory.** Understanding how gear ratios are calculated, different types of gear trains and their advantages/disadvantages, and how stresses act on the gear teeth.

Pre-requisite knowledge will include:

- **FDM.** This is the chosen method of manufacturing. Understanding of tolerances, properties of finished prints, how settings affect print quality.
- **Actuators.** The produced gearbox will be a component of an actuator. What an actuator is, what a servo motor is and how it works.

4.2.2 First Prototype Design

This includes all the tasks that need to be completed to create the first prototype.

Tasks include:

- Using theory to design the performance characteristics of the gearbox. This will include finding the correct gear ratio, the correct number and size of teeth on the gears, and ensuring the output can handle sufficient moment loads.
- CAD modelling of the design
- Manufacturing the gearbox
- Assembling the gearbox (if assembly is possible)
- Testing the gearbox (if assembly is possible)
- Understanding why failures occurred. Were the failures due to incorrect design? Manufacturing problems? etc. (if failures occurred)
- Exploring design improvements.

4.2.3 Dissertation Writing

This will include all the information about the project and discuss how successful it was. Also included will be a discussion on the wider engineering applications of what has been learned. Will conclude with recommendations for an iteration of the design and other ideas to explore.

4.3 Design Specification

Motor

- LHI MT2204II 2300Kv Brushless motor

Power Source

- LiPo 3 Cell Battery. 11.1v, 1800mAh, 20Wh, 75C

Speed Control

- Turnigy Plush 10A ESC. BEC—2A/5V, DC—5.6~ 16.8v
- Quantum 2.4Ghz Remote Transmitter & Receiver

Actuator Constraints

- Maximum actuator dimensions: $100 \times 100 \times 50$ (mm)
- Ideal actuator dimensions: $80 \times 80 \times 40$ (mm)
- The motor, ESC, and receiver must be housed within the specified volume
- Gearbox mass should not exceed 250g

- Must be manufacturable in a typical hackspace
- Actuator manufacture cost must not exceed £50

Performance Requirements

- Maximum actuator output torque must exceed 10Nm
- Actuator must withstand 10Nm of moment loading during operation
- Minimum actuator RPM under 10Nm of load should be greater than 15RPM

3D printer Spec

- Nozzle diameter: 0.4mm



Figure 4.1: Shows the provided equipment to test the gearbox. 1) Transmitter. 2) Receiver. 3) Battery. 4) Brushless DC Motor. 5) Electronic Speed Controller.

Chapter 5

Prototype Design

5.1 FDM Tolerance Testing

Test pieces were manufactured to understand the tolerance range of the 3D printer. This information was used to select the correct tolerances for the prototype design. The test pieces are shown in Figure 5.1. Figure 5.1(A) tests the dimensional accuracy of the printer. Figure 5.1(B) is push fit test, which is used to design the correct fit between printed parts. Figure 5.1(C) tests the detail resolution of the printer.

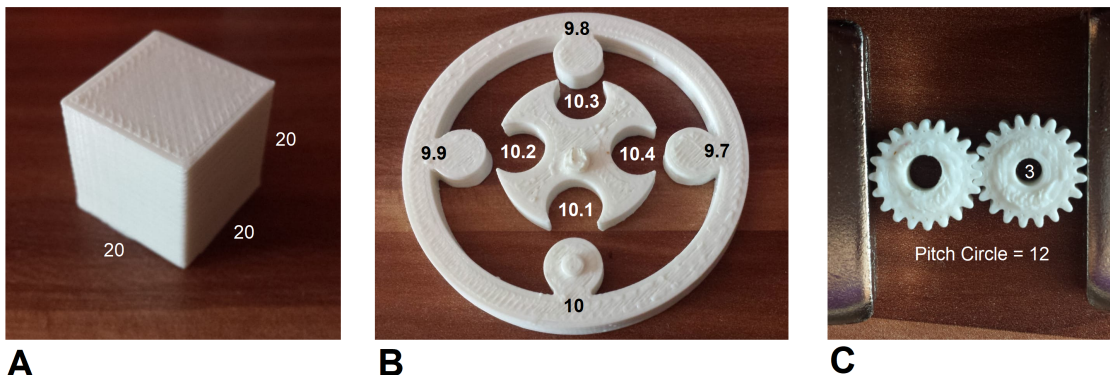


Figure 5.1: FDM tolerance test pieces. All values are the intended measurements and are given in millimetres.

The results of the tolerance test are given in Table 5.1. The dimensional accuracy of the print is higher than expected. The results suggest that the dimensional accuracy does not need to be considered for the prototype design. The fit test was not sufficient enough to determine the correct tolerance for an interference fit—but it was thought that a tolerance of $-.5 \pm .05$ would be a good estimate for an interference fit, given the results. The results of the detail fit were a success overall. The gears were able to mesh and were not malformed.

Table 5.1: Tolerance Test results. All values given in mm units.

Piece	Dimension	Designed Value	Actual Value
A	Length	20	20 ± 0.1
	Width	20	20 ± 0.1
	Height	20	20 ± 0.1
	Diameter Pair	Fit type	Tolerance
B	10-10.1	Transitional	.5 ± .05
	10-10.2	Transitional	.1 ± .1
	10-10.3	Clearance	.15 ± .15
	Successful?		
C	Yes		

5.2 Motor Performance

The performance characteristics of the motor first needed to be known so that the gearbox could be designed correctly for the application. The performance profile of the motor is shown in Figure 5.2. The graphs were produced by working through the equations found in §3.2—using the input values from §5.2.1. The region to the left of the maximum continuous current threshold is where the rate of heat generation does not exceed the thermal rating of the motor (continuous operation).

5.2.1 Motor Specification

The selected motor is an LHI 2204 2300KV Brushless Motor.

- Motor KV 2300KV RPM/V
- Motor Resistance (RM) 0.0951Ω
- Idle Current ($I_o/10V$) 0.6A/10V Max
- Max Continuous Power (W) 180S 190W
- Weight $\approx 26g/0.92oz$ Lipo Cell 2S-3S
- Motor Diameter 27.7mm/1.09in
- Motor Body Length 29mm/1.14in
- Overall Shaft Length 30.6mm/1.2in
- Bolt holes spacing 16mm/0.63in/19mm/0.75in
- Bolt Thread M3x5

Power Supply Specification

The selected power supply for the motor is a TATTU LiPo battery pack.

- 3 Cells
- Voltage 11.1v
- Energy Capacity 20Wh
- Storage Capacity 1800mAh
- Discharge rate 75C
- Dimensions ($L \times W \times H$), $91 \times 33 \times 19$ mm

Motor Performance Charts

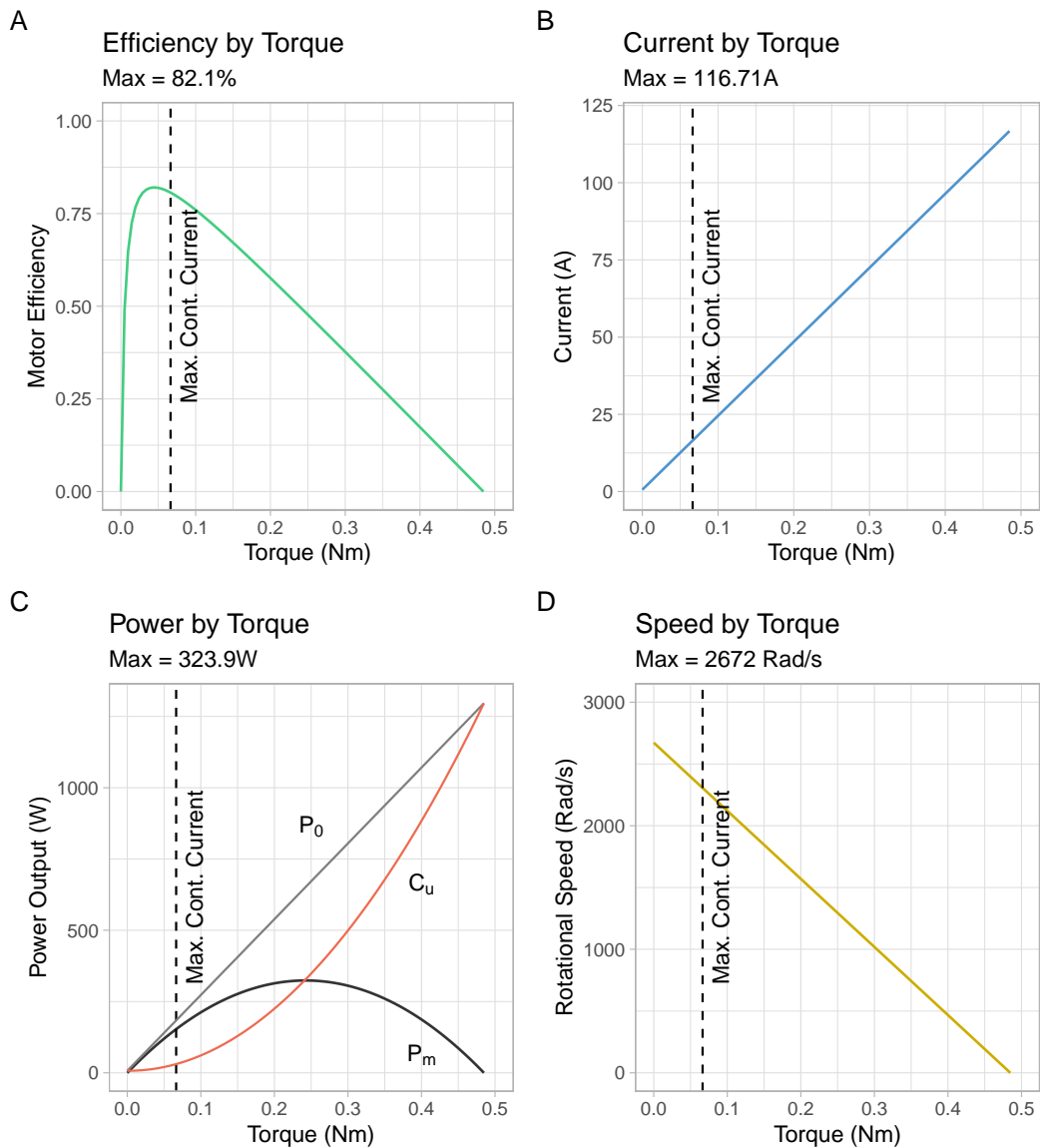


Figure 5.2: Motor performance profile. N.B. $C_u = \vartheta$ (Copper losses).

5.3 Gearbox Design

5.3.1 Gear Ratio Selection

Remember that the actuator must produce 10Nm of torque and a minimum rotational speed of $\pi/2\text{Rads}^{-1}$. To account for mechanical power losses, the value of each requirement was doubled to ensure a sufficient margin of error. The conditions are then expressed mathematically as

$$20 < i\tau; \quad \pi < i\omega. \quad (5.1)$$

The information in Figure 5.2 was used to select τ , ω , and i . The operating efficiency of the motor should be as high as possible. Although it is not necessary for an actuator to run continuously for robotics applications—meaning it is okay for the operating load to exceed the rated (maximum continuous) load—if possible, the operating load should be below the rated threshold to maintain high energy efficiency.

For the initial prototype, a gear ratio of 1024:1 was selected. Reasons for this choice will become clear in the following sections—but the main reason for this choice is due to the high energy efficiency that can be achieved, and also because of the high amount of design simplification (this ratio can be decomposed into five identical 4:1 stages). This particular ratio corresponds to the performance markers of the motor and gearbox shown in Table 5.2. The table shows that the torque condition is met, but the speed condition is not. However, it was thought that the output speed of the gearbox is still sufficiently high to meet the original speed constraint ($\pi/2 < i\omega$) after power losses. Another reason for selecting the high ratio is to lower the maximum unloaded RPM of the output. This improves the rotational precision of the actuator. Also, since PLA has a low maximum operating temperature—if the efficiency is low, then the additional heat generation from the motor could become problematic. Therefore, a high ratio helps to avoid this issue.

Table 5.2: Shows the operating motor performance at 20Nm of load and gear ratio of 1024:1. N.B. The stall torque and no-load speed of the motor and actuator is given for reference.

Parameter	Symbol	Units	Motor Output	Gearbox Output ($i = 1024$)
Stall Torque	τ_0	Nm	0.485	497
No-Load Speed	ω_0	Rads $^{-1}$	2672	2.61
Torque	τ	Nm	0.0195	20
Speed	ω	Rads $^{-1}$	2564	2.50
Current	I	A	5.30	—
Efficiency	ν	—	76.9%	—

5.3.2 Gearing Selection

The two main factors affecting the selection of the gearing are design complexity and available manufacturing methods. Different gear types are suited to different ranges of materials and manufacturing methods. The manufacturing method is limited to FDM and the material selection for the gears is limited to PLA. As a result, worm gears are not thought to be a good choice for gearing—despite having the best space efficiency of any single stage gear—as the resolution of the print layers is likely not to be high enough to ensure smooth sliding between the gears. This could result in large amounts of friction—and thus, significant heat generation. This may affect the mechanical properties of the PLA and reduce the efficiency, or, lead to mechanical failure.

Other types of gearing which can obtain high ratios in a small amount of space are expensive and complex to design—and are out of the scope of this project—thus, are not suitable. This leaves the choice of helical or spur gearing.

Spur gearing was chosen for the first prototype due to the simplicity of the gear design relative to a helical gear. Spur gearing was thought to be sufficient to handle the stresses during the intended application, so the main trade-off is increased noise production for design simplification. As highlighted in §3.1.3, planetary gear sets offer the highest gear ratio for given cross-sectional area. Planetary sets can also be easily designed and manufactured using FDM—making them a good choice for the gearing. An additional benefit to planetary sets is the input and output of a single stage is coaxial.

5.3.3 Gearing Configuration

There are two ways in which the planetary gear stages can be arranged within the gearbox. One is a stack arrangement, the other is a block arrangement. These arrangements are illustrated in Figure 5.3

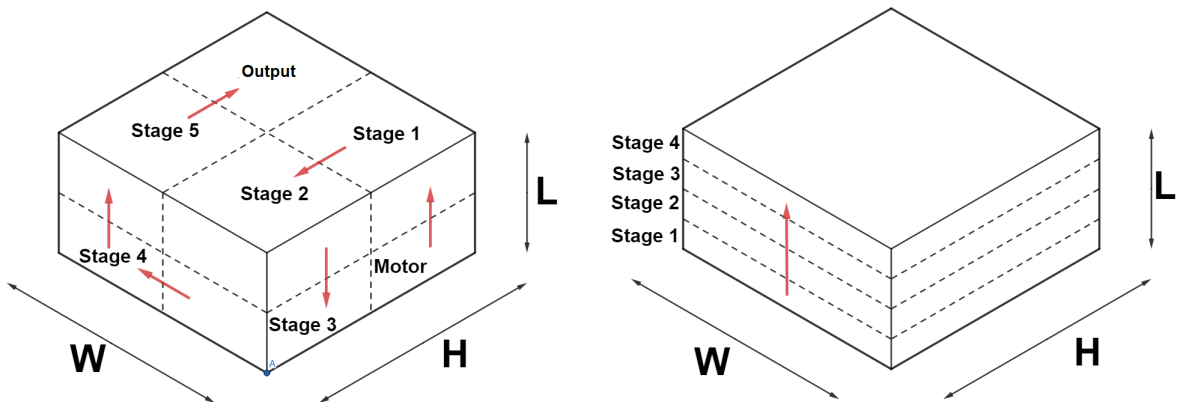


Figure 5.3: Left:- Stack arrangement of planetary stages. Right:- Block arrangement of planetary stages. Red arrows indicate the direction of power transmission through the gearbox.

The advantage of the stack arrangement is that the stages are coaxial—thus, can be directly connected in series. However, this arrangement is not suitable when the length dimension (axial direction) is severely restricted; as is the case with this project. This is due to the thickness of the stage needed to fit the gears and carrier in. A ratio of 1024:1 means that a minimum of four stages are required. With a length constraint of 50mm, each stage would need a thickness less than 12.5mm (not considering any other components)—which is not realistic. Therefore, only low gearbox ratios could be achieved with this arrangement by using one, or possibly two, stages.

The block arrangement is the superior option. This arrangement has room for up to five stages, with room to spare for the motor and output shaft. The width and height for each stage is halved and the length is doubled, relative to the stack arrangement. This results in more favourable dimension constraints for design. The arrangement effectively changes the shape of the available volume from $(50 \times 100 \times 100)$ to $(200 \times 40 \times 40)$; this greatly reduces the design challenge as the effective dimensions are much closer to that of a standard planetary gearhead. The two major drawbacks are that the stages are not coaxial in some cases—so they need to be connected with idle gears—and the maximum ratio of a single stage is 4:1—as with higher ratios, the pinion would be too small. This is the other reason for why an overall gear ratio was selected to be 1024:1—since $4^5 = 1024$ (five identical 4:1 stages connected in series).

Battery Placement

The dimensions of the actuator are ($L=50\text{mm} \times W=100\text{mm} \times H=100\text{mm}$). The gearing, LiPo battery, ESC, and motor must all fit within this volume. The motor fits within the block arrangement and the ESC is small enough to locate within the cavity for the battery wiring—therefore, only the battery needs to be located.

The most simple placement for the battery—given its dimensions—is to locate it at the side of the gearing and to allocate a $50 \times 80 \times 80$ volume for the gearing. The chosen layout for the actuator is shown in Figure 5.4.

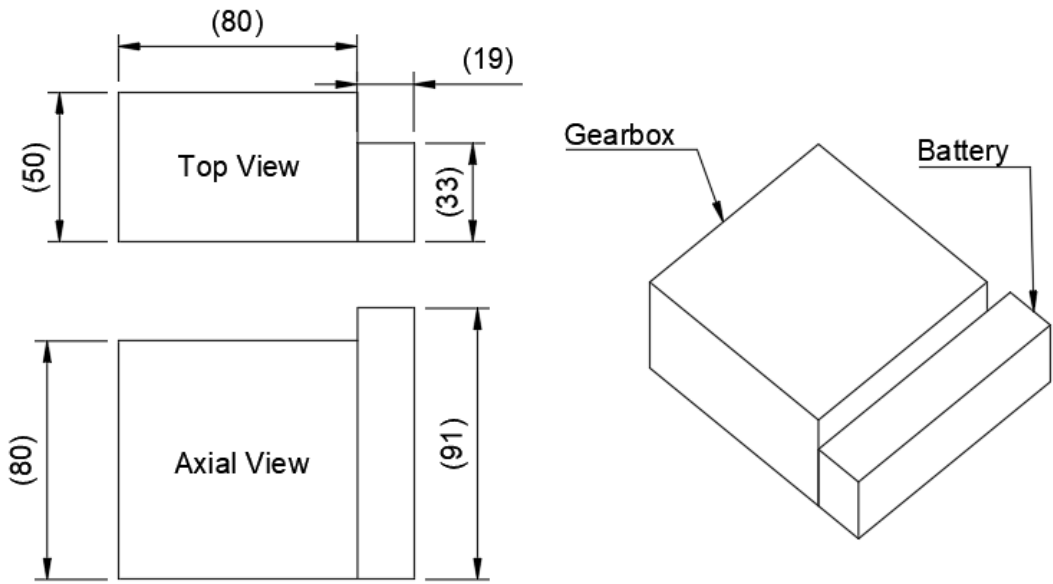


Figure 5.4: Shows the allocated space for the gearbox and battery.

First Prototype Design

The design for the first prototype is shown in Figure 5.5. The battery is not included as the aim of the first prototype was only to test the gearbox function.

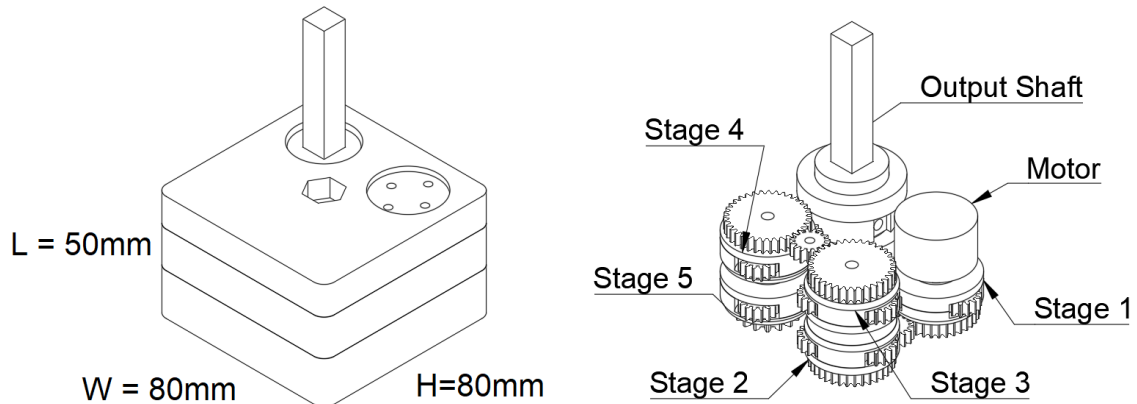


Figure 5.5: First prototype design.

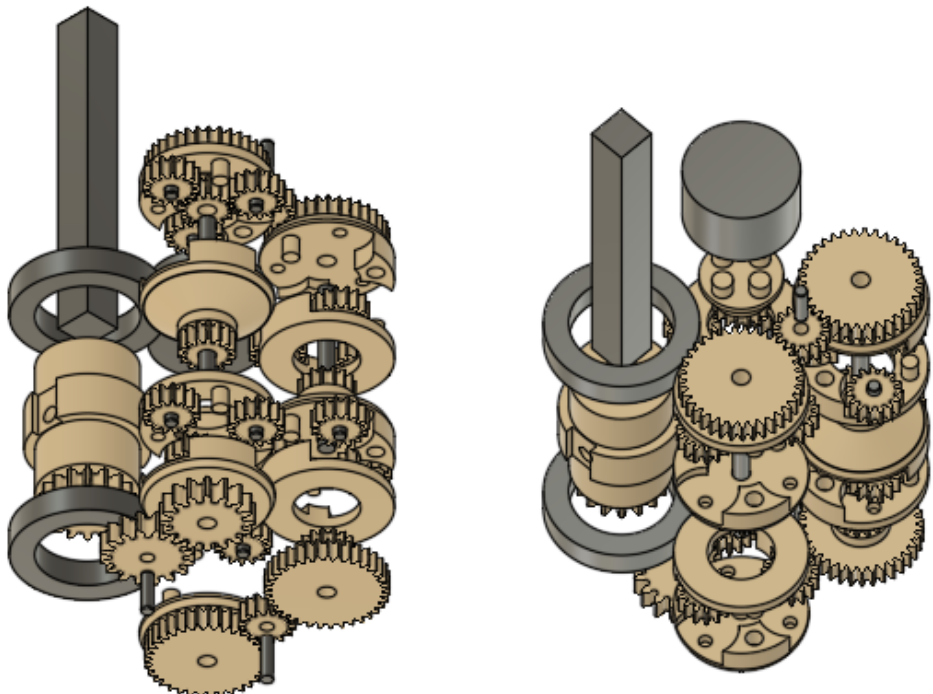


Figure 5.6: Exploded view of the first prototype design.

5.4 Planetary Stage Design

The philosophy of the stage design was to design it such that the same design can be used for all stages in the gearbox. The design also needed to be small enough so that the stages could be arranged in the block formation from Figure 5.3. This implies a maximum side length of 40mm and a maximum thickness of 15mm (to leave space for the idle gears and casing). The main choices for the stage design were as follows:

- The ratio
- The number of teeth on the gears
- The thickness of the gears
- Whether bearings were necessary
- The number of planet gears
- The carrier design
- Tolerances

A rendering of the chosen stage design is shown in Figure 5.9 for reference.

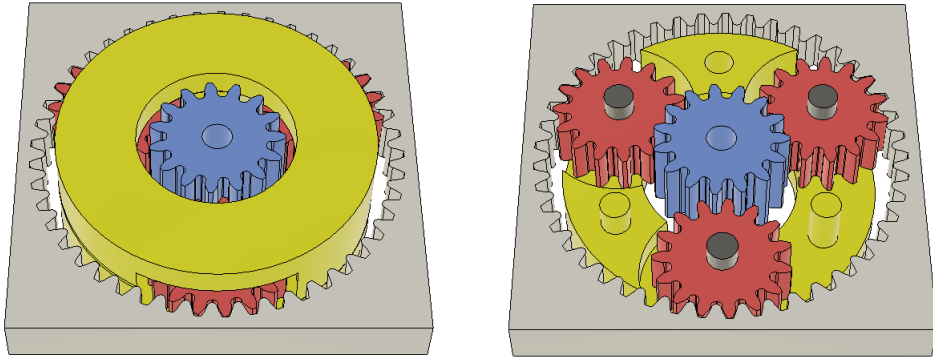


Figure 5.7: Rendering of the chosen planetary stage design.

5.4.1 Gear Design

Shown in Figure 5.8 is a technical drawing of the selected gear design for the single stage 4:1 planetary set. The advantages of this particular design are:

- The side length allows 4 stages to fit within the allocated $80 \times 80\text{mm}$ space for the gearing
- The small diameter of the gears allow the gears to only be 5mm thick, yet still be resistant to wobble. Higher stability implies higher power transmission efficiency.
- The number of teeth on each gear is chosen such that they are large enough to be manufactured with FDM. They are also large enough to handle the maximum load at the output and numerous enough to maintain high power transmission efficiency. This enables the same stage design to be used for all stages.
- The 4:1 ratio is the most space efficient ratio for a planetary set. This enables the gearbox to be small without compromising performance.

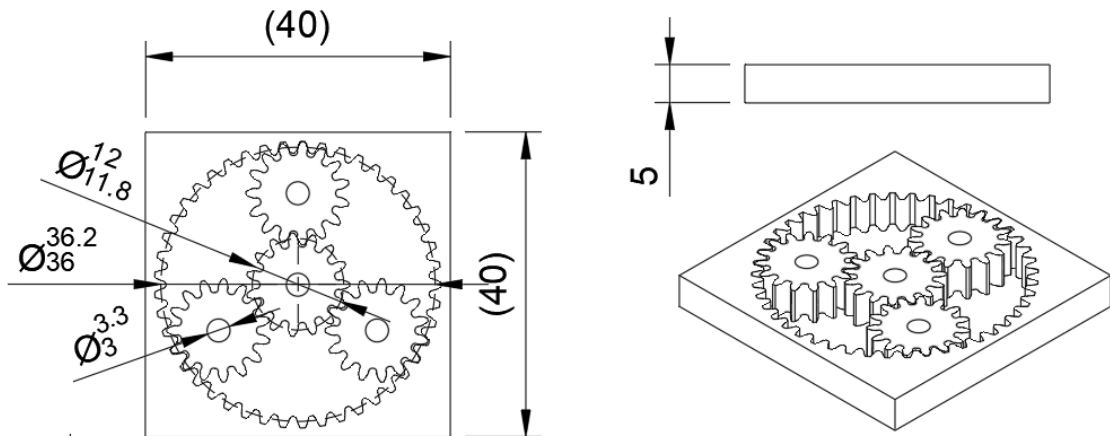


Figure 5.8: Schematic of the 4:1 single stage planetary set for the block arrangement. ($z_r = 45$, $z_s = z_p = 15$). Backlash= 0.15mm. [100]

Ratio Selection

As discussed in §3.1.4—the efficiency of a gear is related to the number of teeth it has. A higher number of teeth on a gear implies a higher efficiency. From Figure 3.6, the ratio with the highest efficiency is a 4:1 ratio. Also, the maximum side length of 40mm for a single stage means that the diametral pitch of the ring gear may be no larger than 36mm. With this space restriction—and only having FDM as a manufacturing option—higher ratios can not realistically be achieved without great difficulty. Since the block arrangement allows the possibility of five identical 4:1 ratios can be connected in series to achieve an overall ratio of 1024:1, it is also not necessary to design the stages with a higher ratio than 4:1. Hence, 4:1 was deemed to be the best choice for the ratio of a single planetary stage.

Planet Number Selection

The carrier could be designed to have either 2, 3, or 4 planet gears, while leaving sufficient space between the gears for the carrier body. Two planets are best for high speed gears as the heat generation is the biggest concern. Having a lower number of planets reduces the heat generation and allows more space for air flow. 4 gears are best when high loading capacity is needed. The load is shared between more teeth. Since the same stage design needed to be used for all stages—some which are high space and others require a high loading capacity—3 planet gears were chosen as a balance between the two.

Gear Thickness

For the chosen gearbox design, each block needed to fit at least one stage, an idle gear, and have space for the casing. The length of a block is 25mm. The casing has a thickness of up to 5mm—leaving 20mm for the idle gear and stage. The idle and stage gears were chosen to have a thickness of 5mm so that 10mm was available for the carrier body while leaving sufficient space for the components to move.

Tooth Stress Analysis

The Lewis equation (§3.1.2—eq.3.5) was used to approximate the maximum tangential load on a single tooth. The input parameters used for the Lewis equation are shown in table 5.3. Here, the value for Y corresponds to the number of teeth $z = 15$. This number was chosen as the maximum number of teeth that the gear could have while maintaining sufficient tooth strength. The UTS of the PLA was estimated to be 60 MPa using the information from §2.2.2.

The Maximum tangential load on a single tooth is then estimated to be 23.2N. A free body diagram of the forces on the planetary stage and the maximum torque each body can withstand without failure of the teeth is shown in Figure 5.9. The diagram shows that the torque of the carrier must not be larger than 1.67Nm. This is below the requirement 10Nm of torque that the gearbox was intended to be designed for. This is

Table 5.3: Input values for the Lewis Equation and the predicted maximum load.

Parameter	Description	Value	Units
F	Face Width	5.00	mm
P	Diametral Pitch	1.25	mm^{-1}
Y	Lewis Form Factor	0.290	—
σ	UTS/3 of PLA	20	MPa
W_t	Maximum Load	23.2	N

the result of a calculation error due to inexperience, which—unfortunately—was not noticed until after the first prototype had been manufactured.

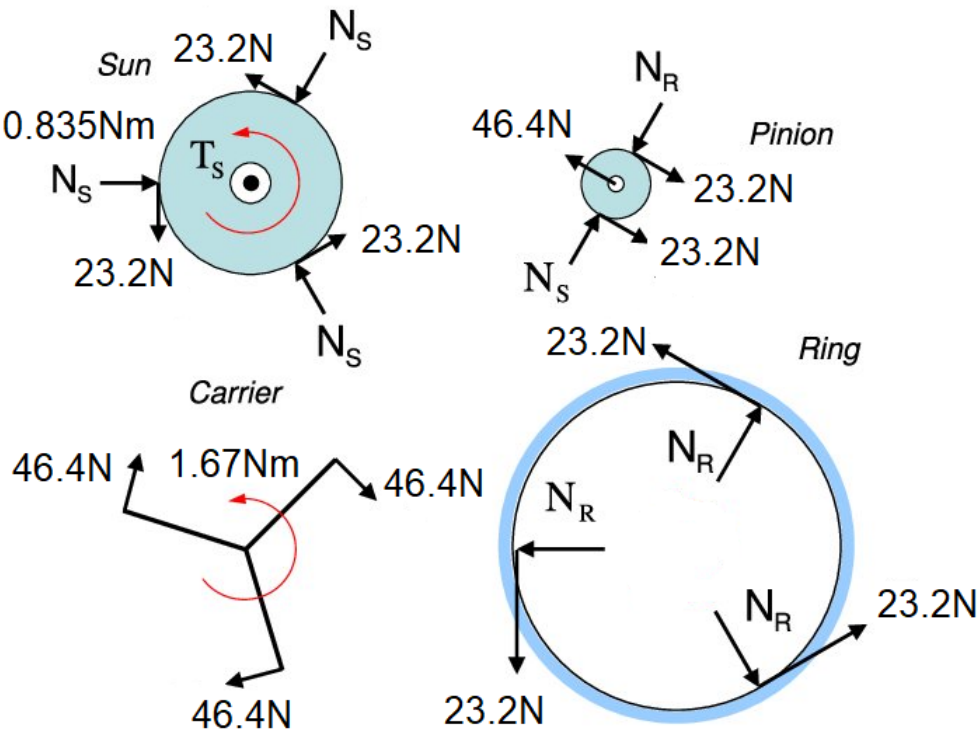


Figure 5.9: Free body diagram labelled with the maximum forces and torques for each body. Original image created by [46].

Bearing Choice

The decision for the bearings was to omit them altogether from the design. Since PLA has a low coefficient of friction, it was thought that the gears could be designed to act also as plain bearings and take advantage of this property. This eliminates the need for ball bearings for each gear. The gearbox would need over 20 bearings—each at a price of around £1—this would have significantly increased the manufacturing cost of the gearbox.

Planetary Carrier Design

A technical drawing of the chosen planetary carrier design is shown in Figure 5.10. The philosophy behind the design was to design the carrier from two identical halves that would hold themselves together using printed pins and holes designed with a push fit tolerance. The printed pins would eliminate the need for fixings to hold the two pieces together.

The two halves would allow the carrier to be printed without the need for support material. A carrier printed from one piece of material would require a significant amount of bridging to create which would result in a large amount of support material that needs to be cleaned. It was decided that the drawbacks were not worth the benefits of a carrier made from a single piece of material.

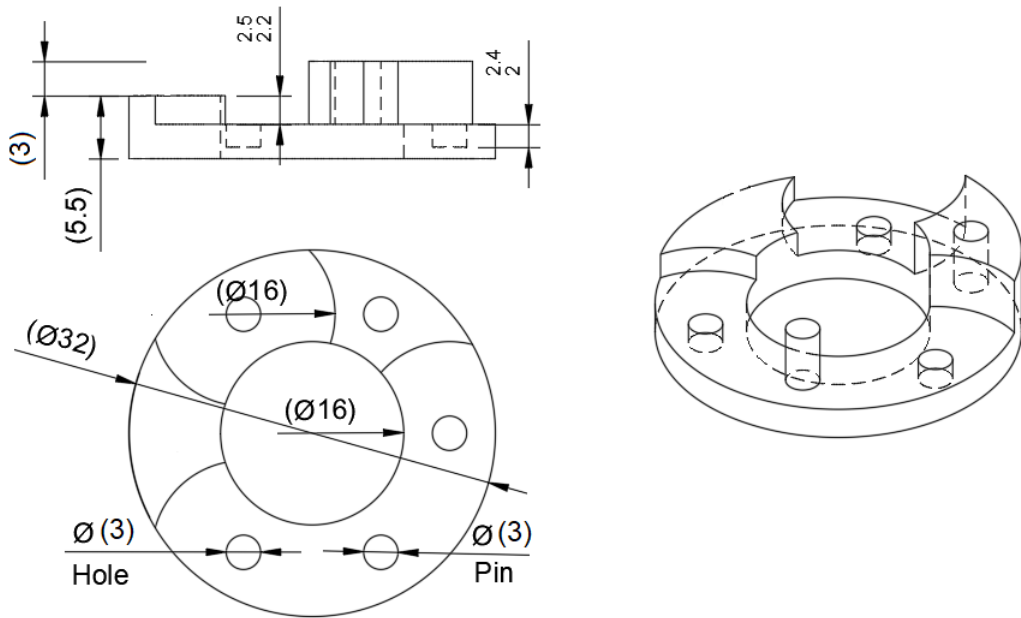


Figure 5.10: The chosen carrier design for the planetary stage.

The holes in the carrier are there to house the gear axles. Steel pins with a length of 8mm and a diameter of 3mm were chosen for the axles.

Tolerance choices

The tolerances were chosen by identifying the type of fit needed and then using the results of the tolerance test accordingly.

The holes in the gears have a tolerance such that the axles should easily thread through the hole and the gear should spin freely. This tolerance is the most important to get right. If the fit is too tight then the friction will result in large power losses. If the tolerance is too loose, then the gearbox will suffer from excessive play. In the event that the tolerance was too tight, the thought was that it would be possible to remove

a small amount of material using a miniature cylindrical file. The main concern was that the tolerance would be too loose.

The backlash for the gear teeth was designed to be 0.15mm. This gives a combined backlash of 0.3mm for two meshed gears. This was chosen as it was thought that making the backlash any larger would be detrimental due to the relative size of the teeth.

The tolerance for the carrier pin and hole were designed to be an interference fit so that the carrier holds itself together without any additional parts.

All other tolerances and measurements were considered not important and so were arbitrarily chosen.

5.4.2 Power Transmission between stages

The design for the power transmission between non-coaxial stages are shown in Figure 5.11. The input and output gears are connected by an idle gear. The input gear is fused to the sun gear and the output gear is fused to the output carrier. The number of teeth and pitch circle diameter of the transmission gears is arbitrary—thus, the size of the teeth and backlash were selected to match the planetary gear teeth. The stresses were calculated to be low enough that the tooth size was not a problem, despite having less gears than the planetary set to share the load with.

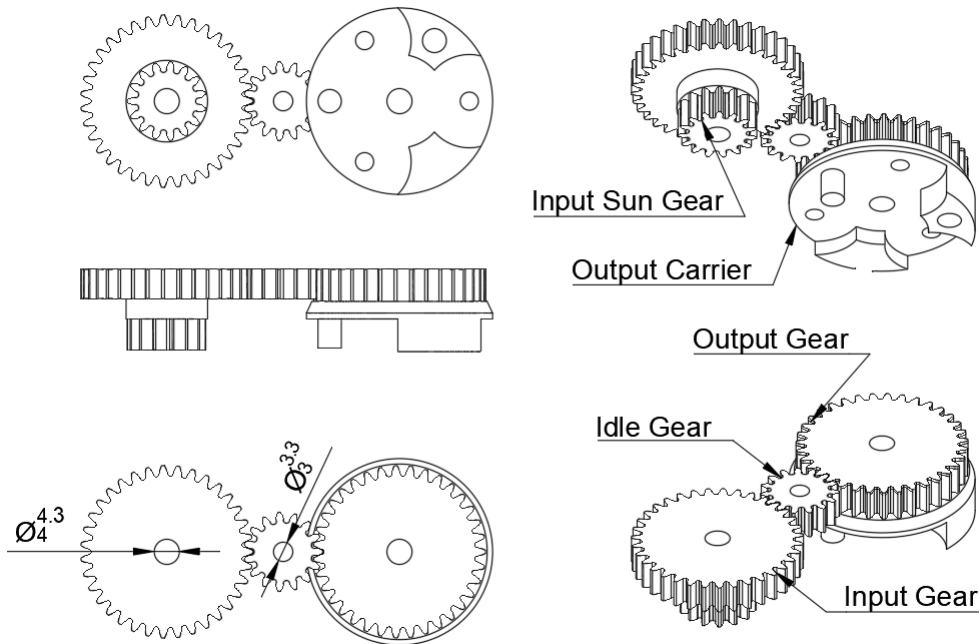


Figure 5.11: Schematic of the power transmission between non-coaxial stages.

5.5 Output Shaft

The design for the output shaft of the gearbox and the power transmission from the fifth planetary stage is shown in Figure 5.12. The output shaft is a $10 \times 10 \times 100$ mm square aluminium rod. The shaft is held within a cylindrical PLA housing and fixed in place with a bolt. The shaft housing is held in place by two PLA bearings on either side of the shaft collar; this allows the shaft to freely rotate. The power is transferred to the output shaft by a set of idle gears connected to the final stage of the gearbox.

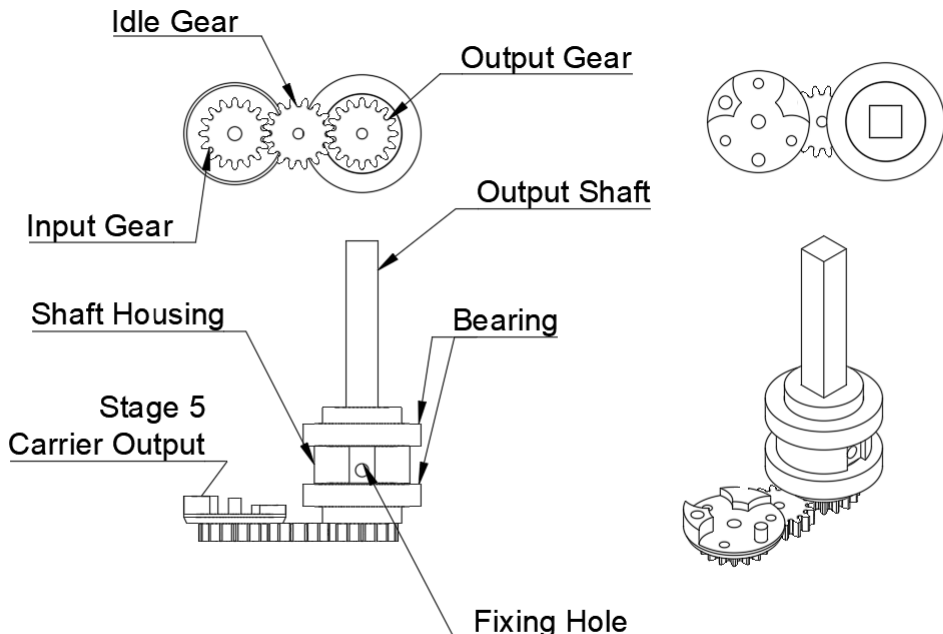


Figure 5.12: Drawing of the output shaft design including the transmission from the stage 5 output.

The transmission gears are the same size and have larger teeth than the other power transmission gear sets. The reason for the bigger teeth is that a single tooth has to be strong enough to withstand the full 10Nm of torque that the gearbox is rated for.

5.5.1 Gearbox Casing

The design philosophy for the casing was to design the casing in such a way so that the gearbox could be assembled layer by layer from the bottom. The advantage of this is that the gearbox could be held together by a single bolt threaded through the centre. Additionally—four steel pins are threaded through all the layers of the casing primarily to stop rotational movement between the layers and to increase structural rigidity. N.B. The casing was only designed to test the function of the gearing, so other—potentially better options—were not explored.

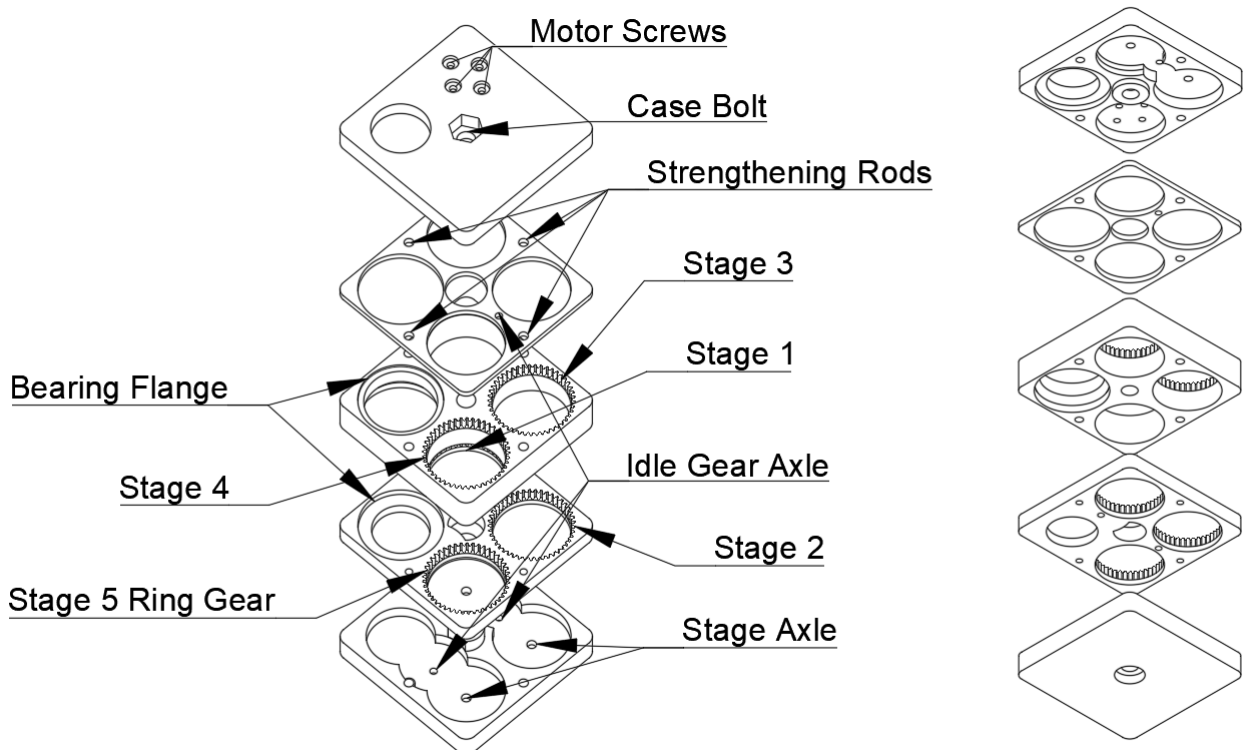


Figure 5.13: Exploded view of the design for the gearbox casing.

The case layers were designed such that minimal bridging was required, which enabled the parts to be 3D printed without the need for supporting material.

The case bolt is a M8 × 45mm cap head bolt with a M8 hexagon nylon locking nut. Both the nut and bolt head are countersunk into the case to prevent interaction with external members. The motor screws are M3 × 6 button head screws; these are also countersunk into the case. The strengthening pins and the stage axles are 45 × 4mm steel pins; these were the cheapest option for pins of that particular length. The idle gear axles are 12 × 3mm steel pins.

Chapter 6

Results

Due to the Covid-19 situation, it was not possible to manufacture all the parts needed for a full working prototype. Therefore—the prototype testing and associated data has been omitted. The results include images of the manufactured parts and an informal test of the function of the PLA bearings.

6.0.1 Manufactured Parts

The manufacturing of the parts had mixed results. The major issue (with all parts that had holes) was that the diameter of the holes were considerably smaller than intended; 0.5mm or more in every case. This caused excessive interference between the mating parts—thus, the parts did not fit together. Due to not having access to the manufacturing equipment, it is not known what the cause of the issue was. After an inspection of the parts, it was thought that the most likely explanation was that the nozzle offset was incorrect.

Aside from this issue, some of the printed parts were generally successful. The parts for the casing—shown in Figure 5.13—would only have required minimal cleaning to be functional. The output shaft, gears, and bearings shown in Figures 6.2 and 6.3 were also fit for purpose.

Some of the manufactured pieces required overhangs in order to be printed as a single piece. The quality of the overhang depended upon the angle. This is illustrated in Figure 6.4. Where the angle was too large, the PLA exiting the extruder nozzle could not find purchase on the previous layer to support it—hence, this is why the overhangs look bumpy in a) and b). Image c) had a much steeper overhang angle and so the overhang print was of a much higher quality.

The unsuccessful prints are shown in Figure 6.5. As mentioned earlier, the holes were consistently smaller by approximately 0.5mm, and the pins were consistently 0.5mm larger in diameter than intended. Also, the tops of the pins were malformed. The thought is that the pins have a small cross-sectional area—so during printing, the previous layers had not sufficiently cooled down before the next layer was deposited. This led to the freshly deposited PLA not holding its shape. The gears shown in c) and d) were also malformed. This could be due to the extruder nozzle moving too fast and

not allowing sufficient cooling of the previous layer. It is assumed that c) was printed before d) and adjustments were made to improve the quality between the two prints.

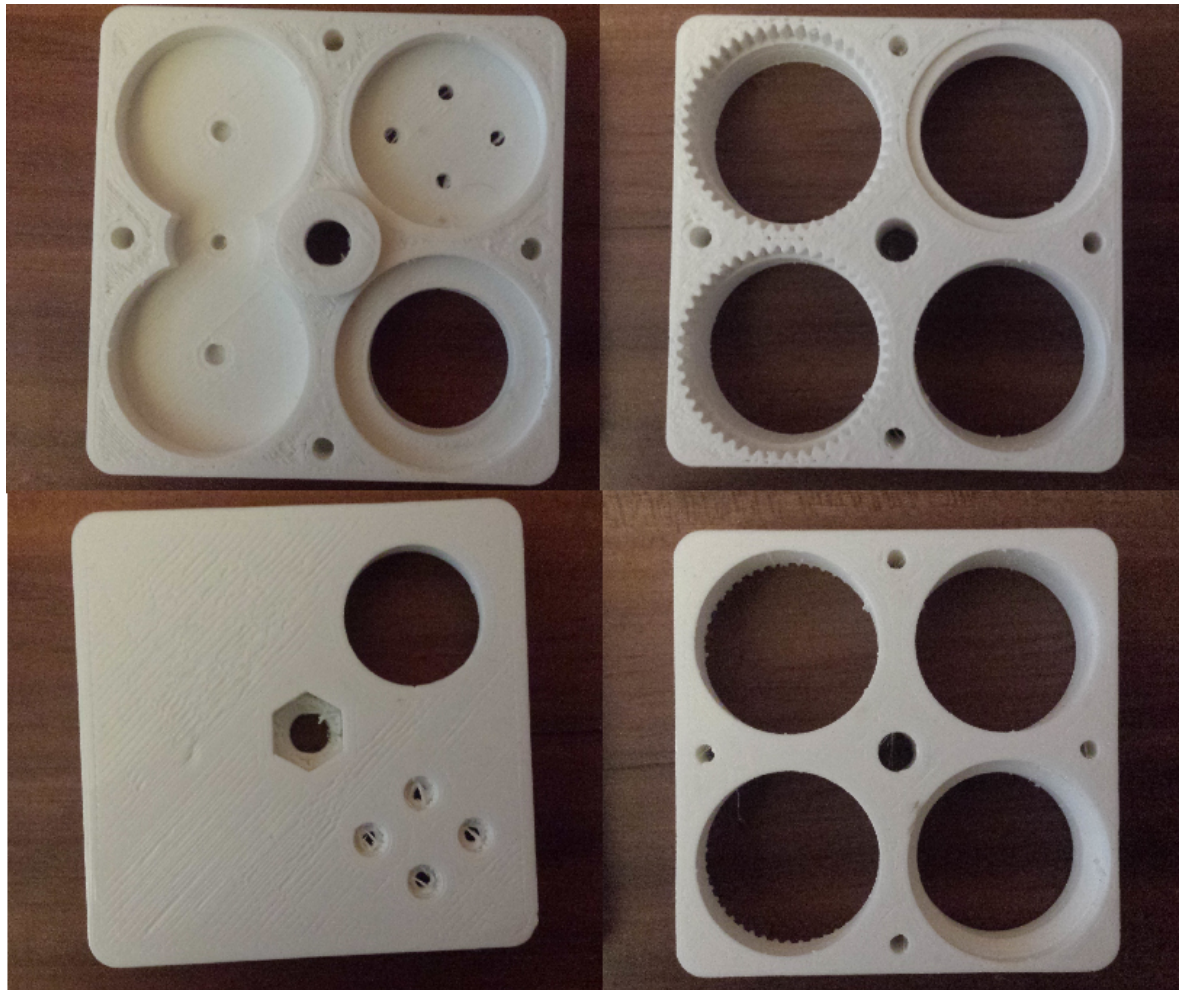


Figure 6.1: Shows examples the front and back of the casing printed parts.

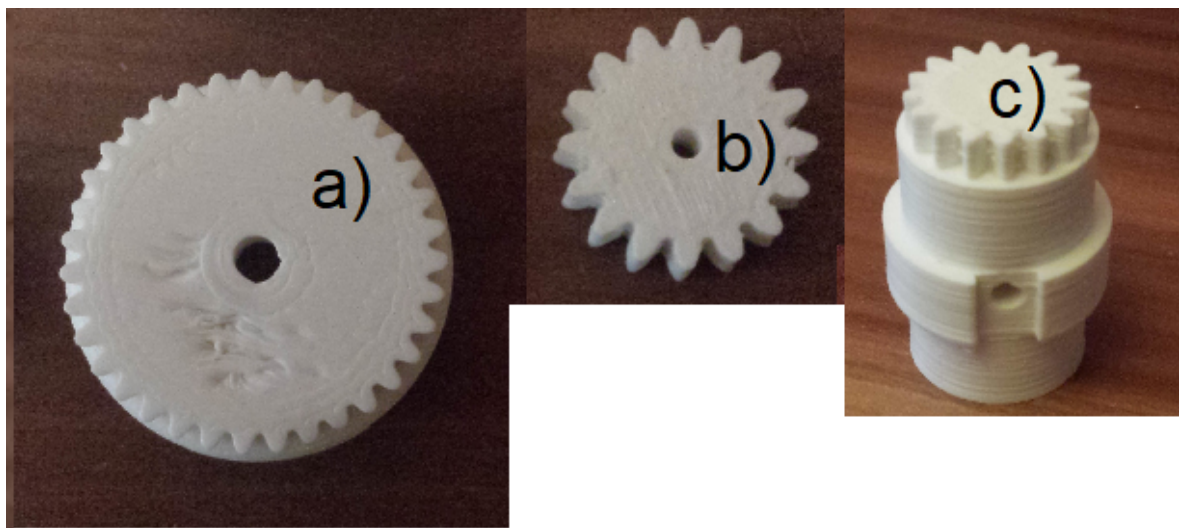


Figure 6.2: Shows examples of the most successful printed parts.

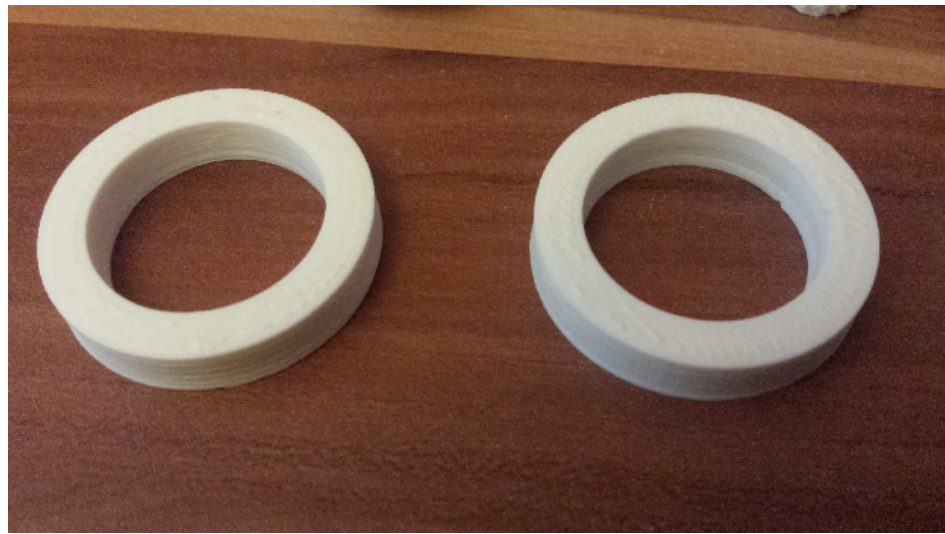


Figure 6.3: Shows the PLA bearings for the output shaft.

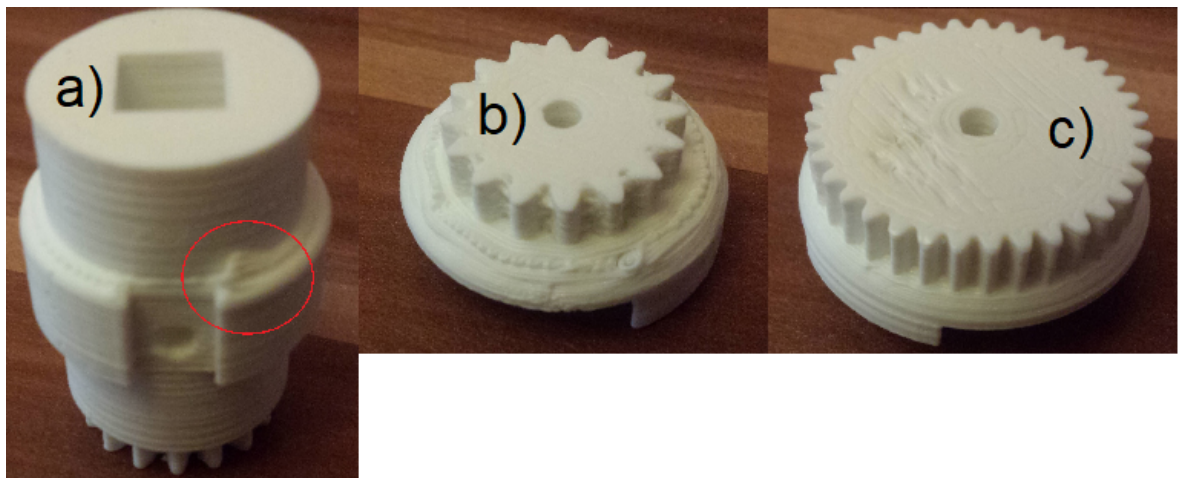


Figure 6.4: Shows examples of overhang print quality for different overhang angles.
Image a): 50°. Image b): 55°. Image c): 30°.

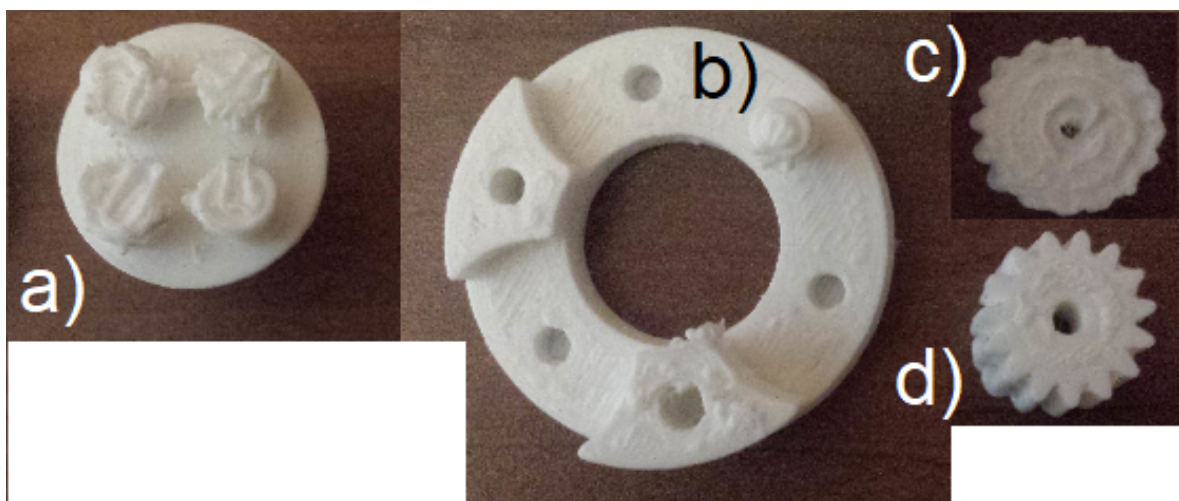


Figure 6.5: Shows examples of components that were printed unsuccessfully.

6.0.2 Bearing Test

Enough of the gearbox could be assembled to informally test the function of the PLA bearings. The assembly is shown in Figure 6.6. The first test was a no-load test to see how easily the output shaft would spin. The shaft was spun with a finger with a small amount of force. The shaft was able to continue spinning for a short period of time after force had stopped being applied—approximately 0.2 – 0.5 seconds. This was enough to show that the bearings did an adequate job at allowing the shaft to spin with minimal friction. At times the shaft did stick. This was due to both small defects in the print and when the bearings were not aligned correctly. After a short time, the defects had less of an effect and it is thought that wearing the bearings in is enough to eliminate this issue. misalignment of the bearings can be solved with manufacturing iteration.

Next was a load test. The end of the shaft with the output gear was pressed into the bearing with a large amount of force and then an attempt was made to turn the shaft. It was difficult to apply the force in a constant manner—but the shaft was considerably harder to turn. However, the shaft was still able to slip. It is thought that with lubrication, the bearing could still function even under a large load.



Figure 6.6: Shows the partly assembled gearbox for the bearing test.

Chapter 7

Discussion

7.1 Results Discussion

7.1.1 Design Pros

Cost

The design has relatively few parts that need to be purchased. The overall cost of the design is £15.94 for the purchased parts, plus £8 for the motor, plus approximately £4 for the amount of PLA filament needed. The total cost is then approximately £28. This is £22 lower than the specified budget. It is also thought that it is possible to bring the cost below £25 after refining the design. Cost-wise, the design offers a good alternative to current actuators on the market at the same price range as it boasts superior performance over other options.

Output Torque

The maximum output torque of the gearbox is only limited by the strength of the gear teeth since the gear ratio is extremely high. Assuming that the teeth were indestructible—the gearbox would offer a theoretical torque of 100Nm while maintaining a power efficiency above 75% (0.1Nm input torque—Figure 5.2). Although this potential could not be tapped with FDM manufacturing—a design inspired by the prototype which is made from steel could potentially find use in robotics that require higher performance and cost effectiveness.

Output Shaft

The design of the gearbox allowed for a robust output shaft design. No formal testing could be done to test the strength of the output shaft—however, an informal inspection gives confidence that the shaft is easily strong enough to handle the 10Nm of moment loading that the design is rated for. Another advantage of this particular design is that should the aluminium part of the output shaft get damaged—the part would be easily

replaceable. While this would likely not be necessary for the PLA gearbox due to the extremely high relative strength of aluminium—a stronger version of the gearbox for heavy duty application may benefit from an easily replaceable output shaft. Such a design may even want the point of failure to be the output shaft if very high moment loads are a risk.

Weight

It was not possible to weigh the prototype as all of the pieces of the gearbox could not be manufactured. However—it is estimated that the weight of the PLA and fixings would not exceed the weight of a typical mobile phone ($\pm 200\text{g}$). The low weight enables the gearboxes to be connected in series for an application such as a robotic arm without requiring a significant amount of the arms power to move the weight of the gearboxes around.

7.1.2 Design Drawbacks

Tooth strength

As mentioned in the stress analysis of the gear teeth (see §5.4.1), a calculation error resulted in a significant overestimation of the tooth strength of the gears. This invalidates the design from a functional perspective. Corrections were made to the calculations. The result of this was that the last stage of the gearbox would need four planet gears and the thickness of the gears would need to be more than 30mm. It was also found that the last stage of the gearbox would reduce the torque enough so that the penultimate stage would require a gear thickness of only 8mm with four planet gears; the remaining stages could then use the original stage design. This implies that the prototype needs a significant redesign in order to successfully meet the specification.

Noise

During the bearing test, it was evident that during operation the gearbox would generate a large amount of noise during operation. Noise during operation can be mitigated to some extent by manufacturing the parts with better precision and lubrication. As mentioned in §2.3.1, using helical gears rather than spur gears may be a sensible option to reduce noise.

7.2 Wider Applications of Findings

It was shown in the literature review that FDM is an incredibly versatile technology—as such, the knowledge that can be gained from designing products to be manufactured using FDM is very valuable due to its wide-reaching applications.

With bearings being the major drive for increasing the cost of a gearbox, it is encouraging to see that there is potential for successfully manufacturing 3D printed bearings.

The bearings have their limitations of course. They will never match the performance of oilite plain bearings or ball/roller bearings—but for low-cost applications that can trade-off some efficiency for eliminating the need for machined bearings, FDM technology shows promising results. Additionally, the ability to design bearings any size and shape perhaps allows for the possibility of retrofitting into existing products as a replacement when a replacement is otherwise difficult to find and very high strength or very low friction isn't required. In fact—FDM technology could also be applied more widely as a method of replacing broken or worn parts on existing products.

The results show that FDM technology has the potential be successfully applied to manufacturing an ambitious gearbox design. There were issues with the manufacturing process which resulted in many of the parts failing to, the issues were not insurmountable. It is believed that the issues could have been resolved through an iterative process to find the right settings and tolerances for each part.

The main drawback of FDM technology is that it is necessary for the designer to have a close relationship with the printer used for manufacturing. The results showed that the tolerances and dimensions could deviate substantially from the intended measurements—and without access to the printer, it was not possible to understand exactly what had gone wrong. This makes it incredibly difficult to manufacture parts with the precision that FDM technology is capable of remotely; it could even be considered pot luck as the operator may not be consistent in setting the printer up each time; so even if the issue is correctly solved, there is still no guarantee that the next attempt will work. Also—depending on the size of the part—it may be necessary to change the settings to ensure the PLA is cooling correctly before the next layer is deposited. For example, a small part may need much higher cooling, as the time taken to print a single layer is much quicker than for a larger part. Given these issues, it is likely that many iterations would be required to achieve the desired results for each component.

It is thought then that FDM technology has its place in low cost manufacturing where strength is not a significant priority. Another interesting prospect of FDM technology, when strength is a priority, would be to use it in tandem with machined metals. Machining and FDM compliment each other well as machined parts offer the strength and precision that FDM parts cannot—but FDM offers the ability to make cheap and complex parts which would otherwise be expensive to machine. Designs which could incorporate machined metal parts embedded in printed parts could offer some unique and interesting low cost solutions to improving existing products.

The knowledge gained on tolerances is also incredibly useful. While the tolerance scales vary depending on the material and manufacturing method—the selection of the appropriate tolerances for a specific material and manufacturing method is universally applicable to other materials and methods. It has also been shown—due to the failures of the prototype design—that is it vital to thoroughly test and understand the tolerance ranges of the selected material and method so that pieces fit together as desired.

7.3 Conclusion

Despite the severe drawbacks of the first prototype design—it is still thought that a second prototype design inspired by the first is possible. There are a few avenues that may be explored which are thought to solve the issues highlighted in the discussion.

The most interesting option would be to explore the use of waterjet cutting to manufacture the gears using steel—then to embed the steel gears within the PLA printed case. This would solve the tooth strength issues and should also make the design of the tolerances easier. The weight of the gearbox would increase as a consequence—however, the stronger teeth would allow the gearbox to utilize much more of its power to compensate. It is anticipated that the cost would not significantly increase by switching to steel gears as the cost of a 1 kg of steel is comparable to the cost of 1 kg of PLA filament.

An alternative option is to stick with FDM to make the gears and redesign the last stages to make the gears thick enough to handle the loaded. It is thought that this would be possible, however, the design is much more challenging than the previous option.

The final option would be to scrap the idea of a block arrangement for the gears and stick to the more traditional stack arrangement. The consequence of this is that the gearbox ratio would need to be severely reduced. Two 8:1 stages in series to make a 64:1 gearbox is thought to be the maximum achievable ratio given the specification. The advantage of this option is that the loads on the gear teeth are reduced significantly due to the increased radius of the planetary carrier.

FDM has its place in creating low-cost alternatives to products. However, due to the low strength of PLA, it is not the best option when the goal is to make something compact that also needs to be strong. Higher strength materials should be chosen instead. The attempt to manufacture a compact and strong gearbox has exposed the weaknesses of FDM technology—but also has showcased the strengths of FDM for manufacturing complex parts where material strength is not an immediate concern. It is thought that using FDM in tandem with other manufacturing methods is a great way to realise the potential of FDM.

References

- [1] Holden.K. *Gear Nomenclature*. (n.d.). Accessed: June, 2020. [Online]. Available: <https://www.slideserve.com/holden/gear-nomenclature>
- [2] SD3D. *PLA Technical Data Sheet*. (n.d.). Accessed: July, 2020. [Online]. Available: https://www.sd3d.com/wp-content/uploads/2017/06/MaterialTDS-PLA_01.pdf
- [3] 3D Matter. *What is the influence of infill %, layer height and infill pattern on my 3D prints?*. (2015). Accessed: August, 2020. [Online]. Available: <https://my3dmatter.com/influence-infill-layer-height-pattern/>
- [4] Cain.P. *The impact of layer height on a 3D print*. Accessed: August, 2020. [Online]. Available: <https://www.3dhubs.com/knowledge-base/impact-layer-height-3d-print/>
- [5] Matweb. *Overview of materials for Polylactic Acid (PLA) Biopolymer*. (n.d.) Accessed: July, 2020. [Online]. Available: <http://www.matweb.com/search/DataSheet.aspx?MatGUID=ab96a4c0655c4018a8785ac4031b9278>
- [6] KHK Gears. *Gear Trains*. (n.d.). Accessed: June, 2020. [Online]. Available: https://khkgears.net/new/gear_knowledge/gear_technical_reference/gear-trains.html
- [7] Weinberg.S. *Planetary Gears a masterclass for mechanical engineers*. (2018) Accessed: July, 2020. [Online]. Available: <https://www.engineeringclicks.com/planetary-gears/>
- [8] Tec-Science. *Fundamental Equation of Planetary Gears (Willis Equation)*. (2018). Accessed: June, 2020. [Online]. Available: <https://www.tec-science.com/mechanical-power-transmission/planetary-gear/fundamental-equation-of-planetary-gears-willis-equation/#:text=Willis%20equation%20for%20planetary%20gears,-The%20Willis%20equation&text=Although%20the%20planet%20gears%20of,gear%2C%20planet%20gear%20and%20carrier.&text=At%20the%20innermost%20point%2C%20the,the%20sun%20gear%20vs.>
- [9] Hatch.R. *Mechanical Backlash: How much is too much?*. (2017). Accessed: July, 2020. [Online]. Available: <https://drivelines.co.uk/mechanical-backlash-much-much/>
- [10] Boston Gear. *Engineering Information*. (n.d.). Accessed: July, 2020. [Online]. Available: https://www.bostongear.com/-/media/Files/Literature/Brand/boston-gear/catalogs/p-1930-bg-sections/p-1930-bg_engineering-info-spur-gears.ashx
- [11] Shigley.J.E, "Spur Gears," in *Mechanical Engineering Design* 2nd ed. New York, NY, USA: McGraw-Hill, 1963, ch. 11, sec. 12, pp. 497

- [12] http://elearning.uokerbala.edu.iq/pluginfile.php/25255/mod_resource/content/1/Lecture%2011%20Design%20of%20%20and%20Helical%20Gears.pdf
- [13] Builton. *Robotics Technology*. (n.d.). Accessed: July, 2020. [Online]. Available: <https://builton.com/robotics>
- [14] <https://www.lord.com/blog/industrial/six-degrees-of-freedom>
- [15] Ismail.B.A. *Explain the Degree of Freedom*. (n.d.). Accessed: July, 2020. [Online]. Available: <http://jf505industrialrobotics.blogspot.com/2013/12/21-explain-degree-of-freedom.html>
- [16] Fjbruzr. *Types of Gears*. (2019). Accessed: July, 2020. [Online]. Available: https://www.reddit.com/r/coolguides/comments/cis9q8/types_of_gears/
- [17] Gaffga.W. *Servomotors*. (2018). Accessed: June, 2020. [Online]. Available: <https://www.kollmorgen.com/en-us/developer-network/servomotors/>
- [18] Mraz.S. *Two-Speed Gearbox Provides High Speed and High Torque*. (2016). Accessed: July, 2020. [Online]. Available: <https://www.machinedesign.com/motors-drives/article/21834992/twospeed-gearbox-provides-high-speed-and-high-torque>
- [19] How To Mechatronics. *How Servo Motors Work & How To Control Servos using Arduino*. (2018). Accessed: June, 2020. Available: <https://www.youtube.com/watch?v=LXURLvg8bQ>
- [20] Direnc. *Feetech FS5103B Standart Servo Motor*. (n.d.). Accessed: June, 2020. [Online]. Available: <https://www.direnc.net/fs5103b-standart-servo-motor-feetech>
- [21] banggood. *FEETECH SCS15 15KG Digital Dual Shaft Metal Gear Large Torque Servo For RC Robot*. (n.d.). Accessed: June, 2020. [Online]. Available: https://uk.banggood.com/FEETECH-SCS15-15KG-Digital-Dual-Shaft-Metal-Gear-Large-Torque-Servo-For-RC-Robot-p-1377354.html?gmcCountry=GB¤cy=GBP&createTmp=1&utm_source=googleshopping&utm_medium=cpc_bgcs&utm_content=lijing&utm_campaign=ssc-gbg-toys-rcdro-ve-newcustom-80-1118&gclid=EAIAIQobChMIR9TgwJnf6gIV5wiICR2hUwFUEAkYBCABEgIld_D_BwE&cur_warehouse=CN
- [22] ServoCity. *Standard Hub Shaft ServoBlock (24T Spline)*. (n.d.). Accessed: June, 2020. [Online]. Available: <https://www.servocity.com/standard-hub-shaft-servoblock-24t-spline/>
- [23] Pick3DPirnter. *3D Printer Parts: Complete List of 3D Printing Components*. (n.d.). Accessed: July, 2020. [Online]. Available: <https://pick3dprinter.com/3d-printer-parts/>
- [24] Pollard.D. *3D Pirnting - Where Did it All Start?*. (2017). Accessed: August, 2020. Available: <https://www.prescouter.com/2017/03/3d-printing-start/>
-
- [26] Cesaretti.G.*et.al.*. "Building components for an outpost on the Lunar soil by means of a novel 3D printing technology," in *Acta Astronautica* Vol.93, 2014. pp 430-450. [Online]. Available: [Actahttps://doi.org/10.1016/j.actaastro.2013.07.034](https://doi.org/10.1016/j.actaastro.2013.07.034)
- [27] Jayakumar. *et.al.* *Manufacturing the Gas Diffusion Layer for PEM Fuel Cell Using a Novel 3D Printing Technique and Critical Assessment of the Challenges Encoun-*

- tered. (2017). Accessed:July, 2020. [Online]. Available: https://find.shef.ac.uk/primo-explore/fulldisplay?docid=TN_proquest1926679906&context=PC&vid=44SFD_VU2&lang=en_US&search_scope=SCOP_EVERYTHING&adaptor=primo_central_multiple_fe&tab=everything&query=any,contains,novel%203d%20print&offset=0
- [28] Zhang.Y, Fan.S, Li.Z, Liu.H. *A novel 3D-Printing Repair of Surface Cracks for Improving the Mechanical Strength.* (2017). Accessed: July, 2020. [Online]. Available: https://find.shef.ac.uk/primo-explore/fulldisplay?docid=TN_ieee_s8279207&context=PC&vid=44SFD_VU2&lang=en_US&search_scope=SCOP_EVERYTHING&adaptor=primo_central_multiple_fe&tab=everything&query=any,contains,novel%203d%20print&offset=0
- [29] Utesena.M, Pernicova.R. *Technology of 3D Print in Field of Renovation of Architectural Structures and Historical Buildings.* (2018). Accessed: August, 2020. [Online]. Available: https://search-proquest-com.sheffield.idm.oclc.org/docview/2092848652/rfr_id=info%3Axri%2Fsid%3Aprimo
- [31] All3DP. *The Rise of 3D Printed Houses.* (n.d.). Accessed: August, 2020. [Online]. Available: <https://all3dp.com/2/3d-printed-house-cost/>
- [32] Carlota.V. *8 Very Promising Bioprinting Projects.* (2020). Accessed: August, 2020. [Online]. Available: <https://www.3dnatives.com/en/bioprinting-projects-3d-printed-organs-070420205/#!>
- [33] Gurdita.A. *The Most Common 3D Printed Prosthetics.* (2018). Accessed: August, 2020. [Online]. Available: <https://all3dp.com/2/the-most-common-3d-printed-prosthetics/>
- [34] Handesign. (n.d.). Accessed: August, 2020. [Online]. Available: <https://www.sculpteo.com/blog/wp-content/uploads/2016/04/Handesign-prosthesys.jpg>
- [35] Neugart. *Multi-Stage Gearbox.* (n.d.). Accessed: July, 2020. [Online]. Available: <https://www.neugart.com/en/planetary-gearbox/multi-stage-gearbox/>
- [36] Horn.H. *Planetary Gears - A Review of Basic Design Criteria and New Options for Sizing* (2012). Accessed: June, 2020. [Online]. Available: <https://www.machinedesign.com/motors-drives/article/21834575/planetary-gears-a-review-of-basic-design-criteria-and-new-options-for-sizing#:text=Single%2Dstage%20planetary%20gearhead%20ratios,normally%20increases%20length%20and%20cost>
- [37] GeoGebra. (n.d.). Accessed: August, 2020. [Online]. Available: <https://www.geogebra.org/geometry?lang=en-GB>
- [38] SD3D. *PLA Technical Data Sheet.* (n.d.). Accessed: July, 2020. [Online]. Available: https://www.sd3d.com/wp-content/uploads/2017/06/MaterialTDS-PLA_01.pdf
- [39] Simplify3D. *Filament Properties Table.* (n.d.). Accessed: August, 2020. [Online]. Available: <https://www.simplify3d.com/support/materials-guide/properties-table/?highlight=abs>
- [40] MakeItFrom. *Polyactic Acid.* (n.d.). Accessed: August, 2020. [Online]. Available: <https://www.makeitfrom.com/material-properties/Polylactic-Acid-PLA-Polylactide>

- [41] SD3D. *PLA Technical Data Sheet*. (n.d.). Accessed: July, 2020. [Online]. Available: https://www.sd3d.com/wp-content/uploads/2017/06/MaterialTDS-PLA_01.pdf
- [42] Vennix.R. *Polyactic Acid (PLA)*. (n.d.). Accessed: August, 2020. [Online]. Available: <https://web.archive.org/web/20120210194852/http://www.matbase.com/material/polymers/agrobased/polylactic-acid-pla/properties>
- [43][49] Pinshape. *10 Advanced 3D Slicer Settings That Will Save Your Prints*. (2016). Accessed: August, 2020. [Online]. Available: <https://pinshape.com/blog/10-advanced-3d-slicer-settings-that-will-save-your-prints/>
- [44] Sommer.E. *The Perfect PLA Print & Bed Temperature*. (2020). Accessed: August, 2020. [Online]. Available: <https://all3dp.com/2/the-best-pla-print-temperature-how-to-achieve-it/>
- [45] Haasbroek.A. *Temperature Stringing calibration Blocks*. (2018). Accessed: August, 2020. [Online]. Available: <https://www.myminifactory.com/item/object/3d-print-temperature-stringing-calibration-blocks-66344>
- [46] Samanuhut.P. *Free Body Diagram of Single Planetary Gear Set*. (n.d.). Accessed: August, 2020. [Online]. Available: https://www.researchgate.net/publication/267491002_Dynamics_Equations_of_Planetary_Gear_Sets_for_Shift_Quality_by_Lagrange_Method/figures?lo=1
- [47] 3DMatter. *What is the influence of infill, layer height and infill pattern on my 3D prints?*. (2015). Accessed: August, 2020. [Online]. Available: <https://my3dmatter.com/influence-infill-layer-height-pattern/>
- [48] Siber.B. *3D Printing Infill: The Basics Simply Explained*. (2018). Accessed: August, 2020. [Online]. Available: <https://all3dp.com/2/infill-3d-printing-what-it-means-and-how-to-use-it/>
- [51] Dejan. *How brushless Motor and ESC Work*. (n.d.). Accessed: August, 2020. [Online]. Available: <https://howtomechatronics.com/how-it-works/how-brushless-motor-and-esc-work/>
- [52] Menin.S. *Why It's Important to Always Use Tolerances*. (2012). Accessed: July, 2020. [Online]. Available: <https://www.designworldonline.com/why-its-important-to-always-use-tolerances/>
- [53] Emiliano.S. *All About The Density of PLA*. (2019). Accessed: August, 2020. [Online]. Available: <https://all3dp.com/2/pla-density-what-s-the-density-of-pla-filament-plastic/#:text=PLA%2C%20or%20polylactic%20acid%2C%20is,or%20wood%2C%20the%20density%20varies>
- [54] TheEngineeringtoolbox. *Metals and Alloys -Densities*. (n.d.). Accessed: August, 2020. [Online]. Available: https://www.engineeringtoolbox.com/metal-alloys-densities-d_50.html
- [55] Howard.A.Bliss (1920). Elements of Applied Electricity. Journal of Electricity. ch.1, p.6.
- [56] Lenz, E. (1834), "Ueber die Bestimmung der Richtung der durch elektodynamische Vertheilung erregten galvanischen Strme", Annalen der Physik und Chemie, 107 (31),

pp. 483494. A partial translation of the paper is available in Magie, W. M. (1963), *A Source Book in Physics*, Harvard: Cambridge MA, pp. 511513.

[57] Lynch.K. *Gear Efficiency*. (2015). Accessed: August, 2020. [Online]. Available: <https://www.youtube.com/watch?v=vVg8jb5vaMI>

[58] Shigley.J.E, "Spur Gears," in *Mechanical Engineering Design* 2nd ed. New York, NY, USA: McGraw-Hill, 1963, ch. 11, sec. 4, p. 464

[59] Q.T.Vinta. *How to Derive the Formula for the Planetary Mechanism Gear Ratio*. (2018). Accessed: August, 2020. [Online]. Available: <https://www.youtube.com/watch?v=9c1CyklAN5A>

[60] KgGear. *Calculation for Planetary Gear Mechanism*. (n.d.). Accessed: August, 2020. [Online]. Available: https://www.kggear.co.jp/en/wp-content/themes/bizvektor-global-edition/pdf/9.9_Calculation-for-Planetary-gear-mechanism_TechnicalData_KGSTOCKGEARS.pdf

[61] Bagad, V.S. (2009). *Mechatronics* (4th revised ed.). Pune: Technical Publications. ISBN 9788184314908. Accessed Auguaat, 2020.